TRIBHUVAN UNIVERSITY

INSTITUTE OF ENGINEERING

PULCHOWK CAMPUS

THESIS NO: 079/MSPSE/012

Stator Inter-Turn Fault Analysis Using Frequency Response Analysis (FRA) Technique

By

Manju Koirala

A THESIS

SUBMITTED TO THE DEPARTMENT OF ELECTRICAL ENGINEERING IN PARTIAL FULFILMENT OF THE REQUIREMENTS FOR THE DEGREE OF MASTER OF SCIENCE IN POWER SYSTEM ENGINEERING

DEPARTMENT OF ELECTRICAL ENGINEERING, PULCHOWK CAMPUS, LALITPUR, NEPAL

April 2025

Stator Inter-Turn Fault Analysis Using Frequency Response Analysis (FRA) Technique

By

Manju Koirala

PUL079MSPSE012

Thesis Supervisors

Dr. Bishal Silwal

Assistant Professor, Department of Electrical Engineering, Pulchowk Campus, IOE, Tribhuvan University, Nepal

Anil Kumar Panjiyar

Assistant Professor, Department of Electrical Engineering, Pulchowk Campus, IOE, Tribhuvan University, Nepal

A Thesis Submitted to the Department of Electrical Engineering in Partial Fulfilment of the Requirements for the Degree of Master's in Power Systems Engineering

The Department of Electrical Engineering

Institute of Engineering, Pulchowk Campus

Tribhuvan University

Lalitpur, Nepal

April 2025

COPYRIGHT©

CERTIFICATE OF APPROVAL

The undersigned certify that they have read and recommended to the Institute of Engineering for acceptance, a dissertation entitled **"Stator Inter-Turn Fault Analysis Using Frequency Response Analysis (FRA) Technique"**, submitted by **Manju Koirala** in partial fulfillment of the requirement for the award of the degree of **Master of Science in Power System Engineering**.

Asst. Prof. Anil Kumar Panjiyar

M.Sc. in Power System Engineering
Pulchowk Campus, Lalitpur
(Supervisor)

Assoc. Prof. Lalit Bikram Rana

Faculty of Science and Technology
Pokhara University
(External Examiner)

Asst. Prof. Dr. Bishal Silwal

Program Coordinator
M.Sc. in Power System Engineering
Pulchowk Campus, Lalitpur
(Supervisor)

Assoc. Prof. Dr. Basanta K. Gautam

Head of Department
Department of Electrical Engineering
Pulchowk Campus, Lalitpur

April 2025

Tel: +977-1-5443081, Email: doee@pcampus.edu.np, Website: www.doee.pcampus.edu.np

Acknowledgement

I would like to express my deepest gratitude to Assist. Prof. Dr. Bishal Silwal and Assist. Prof. Anil Kumar Panjiyar, my thesis supervisor for their invaluable guidance, continuous support, and encouragement throughout this research work. Their expertise and insightful feedback have significantly contributed to the completion of this work. Furthermore, I am also grateful to the entire team of the Department of Electrical Engineering, Pulchowk Campus, for providing the necessary resources and a conducive environment for academic learning and growth.

I am grateful for the opportunity to participate in the student mobility program under the Capacity Enhancement of Electrical Equipment Condition Monitoring and Fault Diagnosis (CEEECoM) project co-funded by the Erasmus+ program of the European Union. This opportunity not only fostered my academic journey but also broadened my perspectives toward diverse cultures and academic traditions.

I am deeply thankful to the Department of Electrical Power Engineering and Mechatronics, Tallinn University of Technology, and to Prof. Dr. Toomas Vaimann, Prof. Dr. Ants Kallaste, and Mr. Muhammad Usman Sardar for their precious suggestions and support throughout this research work.

Lastly, I want to thank my colleagues, classmates, friends, and family for their unconditional love, belief, and support during this challenging endeavor. Their constant support has been the foundation of this academic journey.

This research work would not have been possible without the contributions and support of all those mentioned above, and I am truly grateful to everyone.

Manju Koirala
079MSPSE012

Abstract

Induction motors are fundamental to industrial operations due to their high efficiency, robustness, and cost-effectiveness. However, they are susceptible to faults, among which stator short faults contribute to nearly one-third of total failures. If not detected early, inter-turn faults can escalate into more severe short circuits, leading to disastrous fatal and substantial financial losses. As industries move toward automation, the need for precise and early fault detection techniques is more critical than ever.

Conventional techniques such as MCSA are generally reliable for diagnosing severe faults but often lack the sensitivity needed to spot defects before they escalate. In contrast, Frequency Response Analysis (FRA) offers a more precise, safe, and sensitive approach. This research emphasizes the identification of stator inter-turn faults in a 0.75 kW star-connected cage rotor induction motor. Frequency response data were gathered under various operating conditions using a Keysight impedance analyzer. The stator is represented through an RLC equivalent circuit model, and both Common-Mode and Differential-Mode impedances are examined to distinguish between healthy and faulty states.

An inter-turn fault can be identified by a noticeable decrease in resonance frequency and a drop in impedance magnitude. To quantitatively assess these changes, statistical tools like the CC, ASLE, SD, and MSE are employed. Among these, SD and MSE have demonstrated higher sensitivity, making them particularly effective for precise fault detection.

Keywords: *Condition Monitoring, Frequency Response Analysis, Impedance Analyzer, Differential Mode, Common Mode, Statistical Indices*

Table of Contents

List of Figures

List of Tables

Abbreviations and Acronyms

HF	High Frequency
IM	Induction Motor
FRA	Frequency Response Analysis
SFRA	Sweep Frequency Response Analysis
IFRA	Impulse Frequency Response Analysis
CBM	Condition-Based Maintenance
CM	Condition Monitoring
IEEE	Institute of Electrical and Electronics Engineers
EPRI	Electric Power Research Institute
MSCA	Motor Current Signature Analysis
DM	Differential Mode
CM	Common Mode

Chapter 1 Introduction

1.1 Background

AC machines encompass equipment like motors, which transform alternating current (AC) electrical energy into mechanical motion, and generators, which perform the opposite function by converting mechanical input into AC electrical output. These machines are broadly categorized into two main types: synchronous and induction machines. In synchronous machines, the excitation of the magnetic field is achieved using an external direct current (DC) source. On the other hand, induction machines generate the field current internally through electromagnetic induction in the field windings. Induction machines are also called asynchronous because they rotate at a speed slightly below synchronous speed.

The application area of AC machines is diverse in today's world, ranging from household applications to power generation and manufacturing industries. Synchronous generators constitute a core component of energy generation systems plant, and induction motors are the primary drive of industrial plants. Whether operating independently or as an integral part of a complex system, these machines must operate flawlessly to obtain optimum results. Hence, the performance of these machines should be continuously monitored for the high reliability and consistency of the system.

Machine condition monitoring aims to maintain equipment by evaluating its previous and current performance. To assess the operational status of a machine, various sensors and instruments are strategically placed around it to gather essential data. Once the data is collected, it is analyzed to support informed decisions regarding maintenance strategies or necessary corrective measures. The approach to machinery condition maintenance relies on aspects like the kind of machine used, the extent of any detected faults, and the potential impact these issues could have on the broader plant operations[1].

Due to various working conditions such as improper installation, poor working environment, thermal, electrical, and mechanical stresses, faults arise in induction machines. These faults are generally categorized into mechanical and electrical types. Faults related to bearing condition and eccentricity fall under mechanical faults, and faults related to stator and rotor fall under electrical faults. There are various techniques

to detect such types of faults for continuous monitoring of the system. The MCSA technique is useful for BRB fault detection of stator short-circuit failures. Vibration signal analysis is suitable for detecting mechanical faults in the machine. For large machines, the partial discharge method is appropriate to detect faults related to insulation failures, which is not suitable for small machines that are fed from adjustable speed drives. The inter-turn fault can be efficiently diagnosed with the Frequency Response Analysis (FRA) technique is widely used to detect the early stages of stator short circuits.

1.1.1 Maintenance Techniques of Electrical Machines

Electric motors play a vital role in everyday life, finding applications in industries, transportation, building ventilation systems, and electronic cooling mechanisms. Among them, induction motors are especially important due to their reliability and efficiency in industrial settings. Nonetheless, harsh environmental conditions in industrial areas can negatively impact their performance, leading to a higher risk of faults. Several factors may contribute to motor failure, including poor design, low-quality components or workmanship, incorrect installation, and adverse operating conditions. To reduce the likelihood of failure and enhance the machine's operational life, regular monitoring and maintenance are essential. Generally, maintenance strategies are grouped into three main categories: reactive maintenance, preventive maintenance, and predictive maintenance[2].

Planned maintenance offers numerous advantages that contribute to the overall efficiency and reliability of equipment. By scheduling maintenance activities in advance, organizations can reduce unexpected breakdowns, extend the lifespan of machinery, and enhance operational safety. It also allows for better resource allocation, minimizes costly emergency repairs, and helps maintain consistent production output. Additionally, planned maintenance supports compliance with safety and regulatory standards while promoting a proactive approach to asset management.

a) Reactive Maintenance

It is also known as breakdown maintenance, as it is performed after the complete failure of the machine. When no maintenance is performed on a machine and it is simply replaced upon failure, this approach is typically suited for non-critical assets within a plant. It is appropriate in cases where equipment failure does not have a significant

effect on overall operations or productivity. Excessive machine downtime, reduced production availability, increased reliance on spare parts inventory, and elevated overtime labor costs are common challenges associated with unplanned maintenance and unexpected equipment failures.

b) Preventive Maintenance

This technique is also called periodic maintenance, as it is done periodically with constant frequency to prevent unexpected failures. Some components are replaced, and only critical assets undergo preventive maintenance due to increases in maintenance costs.

c) Predictive Maintenance

This maintenance approach is carried out according to the actual condition of the machine, which is also called condition-based maintenance. For this, health monitoring instruments and systems are installed in a plant. It is suitable for critical assets, where minimizing downtime and optimizing maintenance schedules are critical for maintaining the reliability of the system. It is a more economical maintenance technique among others on a long-term basis. The advantages of this approach include reduced maintenance expenses, decreased frequency of equipment failures, minimized repair-related downtime, extended machinery lifespan, and enhanced safety for operators.

1.1.2 Condition Monitoring Technique

Condition Monitoring (CM) is a maintenance strategy that involves planning maintenance activities based on the actual condition data collected from the equipment. It relies on specialized software tailored to specific machinery, where the system structure is predefined, and real-time condition data from the plant is continuously fed into the software for analysis. The condition monitoring (CM) software compiles the collected data and presents it in a structured format, enabling maintenance engineers to effectively plan and schedule equipment shutdowns[2].

The growing adoption of automation systems in industrial plants, coupled with a reduced direct interaction between operators and machinery, has heightened the importance of condition monitoring (CM). CM involves tracking and analyzing machine parameters through graphical trend analysis, allowing for early detection, diagnosis, and resolution of potential issues before a failure occurs[3].

1.1.3 Importance of Condition Monitoring

Continuous monitoring of an electrical machine's operating conditions enables early fault detection and facilitates targeted maintenance planning of the maintenance to avoid catastrophic failures is condition monitoring of the electrical machines[4]. Ensuring the reliability and efficiency of electrical machines heavily depends on effective condition monitoring. This includes

1. Preventing catastrophic failures and significant damage to the machines.
2. Stopping unscheduled outages.
3. Optimization of machine performance.
4. Reducing repair time and spare parts inventory.
5. Lengthening of the maintenance cycle.

The advantages of condition monitoring include[3]:

i. Enhanced machine availability and operational performance
ii. Minimization of secondary or consequential damage
iii. Extended service life of the machine
iv. Lower inventory requirements for spare parts
v. Decreased reliance on unplanned or breakdown maintenance

1.2 Problem Statement

Despite their rugged construction, induction motors are susceptible to a range of faults. In industrial settings, stator-related issues account for approximately one-third of all AC machine failures, with nearly 85% of these linked to insulation breakdown. Typically, stator insulation failure originates from inter-turn faults, which introduce additional thermal stress and can progressively damage the insulation system. If the machine is not promptly disconnected from the power source, the fault may escalate and compromise the ground wall insulation. This issue is more prevalent in motors operated with adjustable speed drives, as the presence of high-frequency voltage spikes between turns can trigger partial discharges. Such faults are often early indicators of insulation aging and deterioration. The MCSA is a common and mostly used approach to detect by analyzing electrical signals in induction motors. Its use is not recommended for the detection of stator inter-turn faults as it cannot detect early-stage faults.

Frequency response analysis is suitable for induction motor inter-turn fault detection as it can detect early-stage faults by analyzing the impedance frequency response for a wide frequency range.

1.3 Objective

The objectives of this study are

i) to obtain the impedance response of a healthy motor for a sweep of the frequency from 10Hz to 120MHz
ii) to analyze the stator inter-turn faults by comparing the impedance responses of healthy and faulty machines
iii) to characterize the induction motor in high-frequency operation
iv) to validate the effectiveness of FRA for fault detection by quantifying the results obtained by using statistical indicators

1.4 Scopes and Limitations

This research aims to identify stator inter-turn faults by analyzing the insulation's frequency response over a wide frequency range. A high-frequency model of the induction motor will be created and validated through experimental testing on a specialized test bench setup. In previous research works, distorted flux distribution by inter-turn fault and inter-turn fault detection through DQ modeling of the machine was done. The Parks' Vector approach, integration with MCSA, and Negative Sequence currents are used as detection tools for insulation degradation of a stator winding. There were some works done in frequency response analysis also, but those were performed through experimental works only; the high-frequency modeling of the machine for inter-turn fault has not been done yet.

This study concentrates on identifying stator inter-turn faults, which represent the initial stage of stator short-circuit failures. If not promptly addressed, these faults can escalate into more serious problems, such as phase-to-phase or phase-to-ground short circuits, which may lead to substantial destruction of the motor. For high-frequency modeling of a stator of a motor, equivalent RLC modeling will be used, for which many considerations have to be made.

In this study, the use of deep learning or machine learning is not done, though some statistical indicators are calculated. Till now, it is an offline technology that is

invasive. By integrating machine learning techniques, it can be developed as an online monitoring method for fault detection.

1.5 Thesis organization

This dissertation is organized into five chapters. This section gives a brief outline of each chapter and the contents of each has.

- This chapter gives a background of the dissertation. The problem statement is described, followed by the aims and boundaries of the thesis work.

- Chapter 2 explores the required literature review done for the dissertation, including the fundamentals of induction motors, different types of faults, stator construction, the insulation degradation mechanism of a stator, and the short circuit faults that occur in the stator. This chapter highlights the importance of early detection of stator inter-turn faults through frequency response analysis. It discusses the causes and effects of short circuit faults in the stator, as well as the role of frequency response analysis in reliably identifying early-stage faults and maintaining machine performance.

- Chapter 3 describes the research methodology of the dissertation, including the modeling approach used, experimental setup, and the workflow of the thesis.

- Chapter 4 discusses the obtained results from the model and experiment and shows the reliability of the chosen method.

- Chapter 5 concludes the research work.

Finally, this thesis will end with a list of references that were used while carrying out the research.

Chapter 2 Literature Review

2.1 Induction Motors

Among the various types of rotating electrical machines, induction motors are among the most commonly used types of motors. They are commonly employed in industrial manufacturing, commercial systems, household appliances, and more recently, in electric vehicles. Their popularity stems from advantages such as low maintenance requirements, high reliability, compact size, simple control mechanisms, and high efficiency. An induction motor primarily consists of three key components: the magnetic core, the stator, and the rotor. The magnetic core is made up of multiple thin, insulated steel layers stacked together to create a closed path for the magnetic flux. Its primary function is to effectively conduct the magnetic flux. The rotor, which is the rotating component, is mechanically linked to a shaft that drives a connected load by delivering the necessary mechanical torque. The stator winding is a stationary component that generates magnetic flux within the core[5]. The scattered view of a squirrel-cage IM is depicted in Figure 2.1.

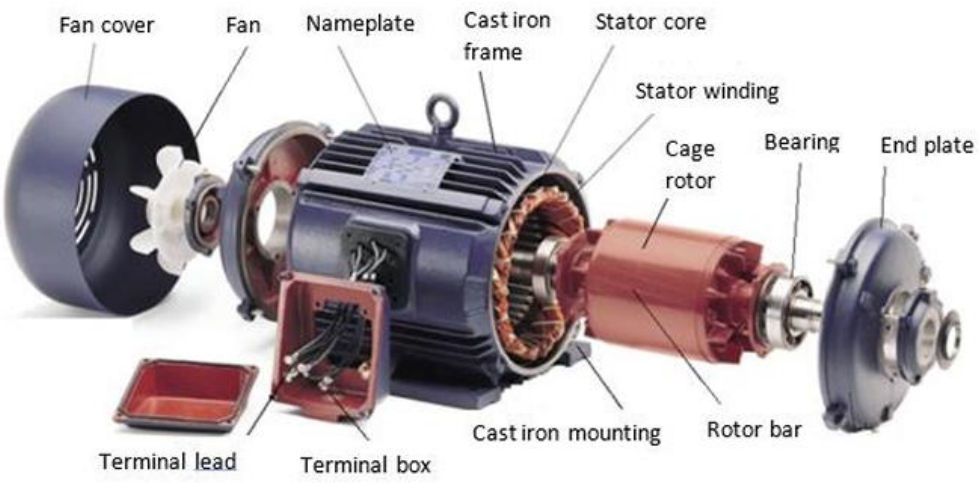

Figure 2.1 Scattered view of the squirrel cage IM structure[6]

2.2 Operating Principle of Induction Motor

An induction motor operates rooted in Faraday's electromagnetic induction law, converting electrical energy into mechanical energy. There is a stator, which is the stationary part, and it carries conductors to supply power. There's also a rotating part called a rotor, which rotates with the help of induced electromotive force. When an AC

signal is supplied to the stator of an induction motor, it creates a rotating magnetic field that moves at a speed known as the synchronous speed, Ns, given by,

$$Ns = \frac{120*f}{P} \quad (2.1)$$

where,

Ns = synchronous speed

f = supply frequency

P = number of pole pairs

The rotating magnetic field interacts with the rotor conductors, generating an induced voltage in the rotor. Consequently, the rotor rotates at a speed slightly less than the synchronous speed. The lagging amount of speed is called slip, which is given by,

$$s = \frac{Ns-Nr}{Ns} * 100\% \quad (2.2)$$

where,

s = slip

Nr = rotor speed

Ns = speed of rotational magnetic field (synchronous speed)

If the rotor were to rotate at synchronous speed, there would be no relative motion between the rotor and the rotating magnetic field, resulting in no induced electromotive force (EMF) or torque.

At low frequencies, the voltage is uniformly dispersed across the stator winding turns. In the medium-frequency range, the motor's behavior exhibits a combination of capacitive and inductive behavior, while at high frequencies, the motor model predominantly displays a capacitive response[7].

Being the primary driver of various industrial applications, the squirrel cage induction machine consumes most of the power in industrial plants. Induction motors, particularly squirrel-cage types, account for about 85% of electrical machines used in industry. During their operation, these machines are susceptible to several faults, including broken rotor bars, excessive air gap eccentricity, bearing wear, and stator winding short circuits. Preemptive detection of faults is crucial for the protection of the induction machine from permanent damage, which also reduces maintenance time and financial losses.

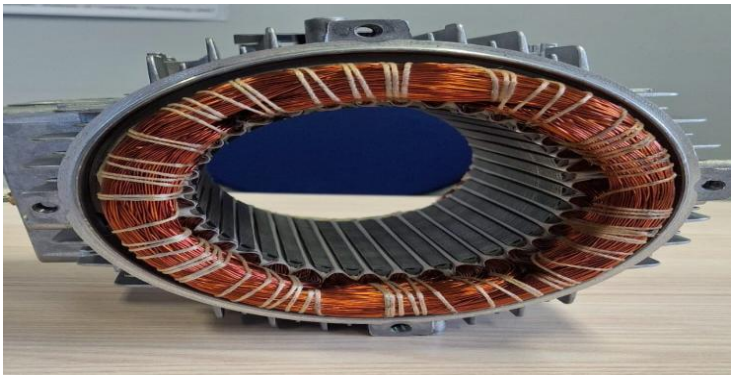

Figure 2.2 Showing the stator of the motor used for the experiment

2.3 Construction of Stator Winding

The stator winding is made up of several layers of insulated copper conductors wrapped around the magnetic core's teeth. This is accomplished by placing individual coils or bars into the stator core, which are then arranged in parallel or series to complete the winding. To avoid contact between the high-voltage conductors in the center and the grounded core, the stator coils and bars are constructed from copper and are insulated[5]. Depending upon the voltage rating, stator windings of different designs are used. For higher-rated machines, conductors of high current carrying capacity are needed, for which conductors of large cross-section are required, which are made from several strands connected in parallel. A thin layer of insulation must be applied between each strand. The stator of a typical squirrel cage IM is shown in Figure 2.2.

2.3.1 Strand Insulation

The use of a greater number of strands of lower cross-sectional area to conduct the necessary current has both electrical and mechanical advantages. The bending of such strands is easy, and also the use of such stranded conductors reduces circulating current losses in the induction machine. The main conductor is made up of many tiny strands connected in parallel to increase efficiency and lower I^2R losses. To preserve their electrical advantages, the strands need to be isolated from one another, have acceptable thermal qualities, and be able to tolerate only a few volts.

2.3.2 Turn Insulation

For medium-sized machines, the stator conductors are made of coils that are connected in series. The turns must be insulated from each other to prevent them from short-circuiting. This insulation system is called turn insulation.

2.3.3 Main or Ground-Wall Insulation

The primary set of electrical paths is electrically separated from the stator core by an insulation system referred to as the main insulation. This insulation is specifically engineered to endure the complete operating voltage of the rotating machine.

2.4 Faults in Induction Machine

Numerous studies indicate that stator failures account for between 30 and 40 percent of induction machine failures. These failures can have disastrous consequences, including unplanned shutdowns and high maintenance costs. To avoid catastrophic IM failures and associated side effects, stator problems must be detected accurately and early.

Electrical machines' faults can generally be divided into two main categories: mechanical and electrical faults. Mechanical faults encompass issues such as bearing-related problems and eccentricity-related faults. Bearing faults can include wear in ball or roller bearings, misalignment, and contamination. Eccentricity-related faults are classified into static and dynamic eccentricities. Failures in the stator may manifest as inter-turn, coil-to-coil, phase-to-phase, or phase-to-ground failures. Rotor-related faults, including BRB and end ring faults, are also common. The primary cause of these failures is the breakdown of insulation in the stator windings, which is induced by various electrical and mechanical stresses. If an inter-turn fault goes undetected, it may evolve into a phase-to-phase or phase-to-earth fault, leading to substantial maintenance costs[8].

According to a study conducted by IEEE and EPRI, different faults in induction motors are shown in Figure 2.4[4]. From Figure 2.4, it is seen that the stator faults constitute about 37% of the total faults occurring in an induction machine. Although new short circuits in the stator windings won't have a big impact on the rotating machine's performance, they can develop quickly and seriously harm the machine. Initial identification and correction of such defects are essential[9]. An inter-turn fault

is difficult to recognize by the classical method until it is severe enough to cause windings to burn and produce a lot of heat.

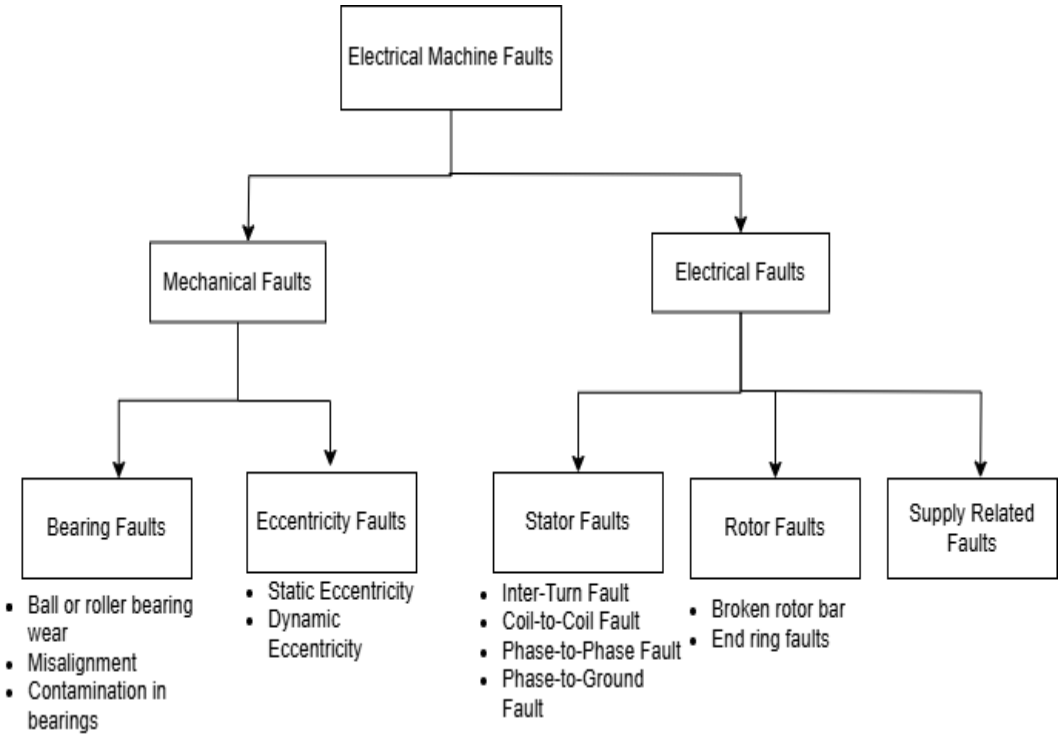

Figure 2.3 Classification of Faults in Induction Motors

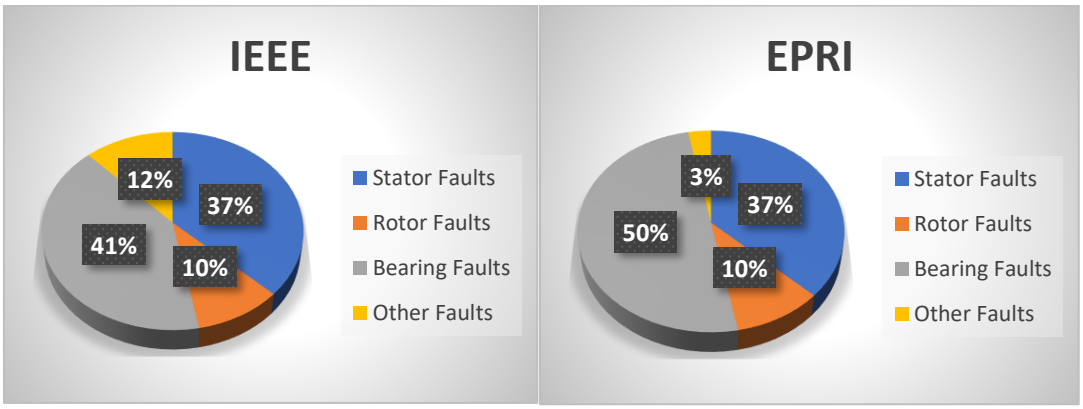

Figure 2.4 Statistics of different faults in IM according to IEEE and EPRI

2.5 Stator Winding Insulation Breakdown Mechanism

For an induction motor powered by an inverter, winding insulation faults are common and are considered serious because they can result in high fault current, production of heat, damaged windings, scorched motors, and, in the most severe cases,

fire dangers. Conductors of stators are surrounded by thin insulation, so this insulating material could be degraded more easily and may be affected by thermal, mechanical, electrical, and ambient (environmental) stresses. When the stator winding's temperature exceeds the threshold temperature limit, insulation oxidation occurs which makes the insulating material brittle, and the copper conductor inside the insulator also gets expanded, damaging the coated insulating material. When machines are operated by inverter-fed drives, the inverter's pulse-width modulation (PWM) can induce surge voltages in the motor windings. Environmental factors, including factors like moisture, excessive humidity, and oil from bearings, dirt from the environment, etc., encompass multiple stresses to the motors[5].

Stator winding insulation faults are generally classified into four main types: primarily as inter-turn (within the same phase), phase-to-phase (between two different phases), and phase-to-ground faults[3]. By identifying inter-turn shorts quickly while the electric motor is running, damage to nearby coils and the stator core would be prevented, lowering repair expenses and motor outage duration[10]. An inter-turn short circuit failure starts when the insulating layer between adjacent stator coils in the stator assembly slot deteriorates, leading to a short circuit. This can result in localized overheating, potentially leading to further damage within the winding system.

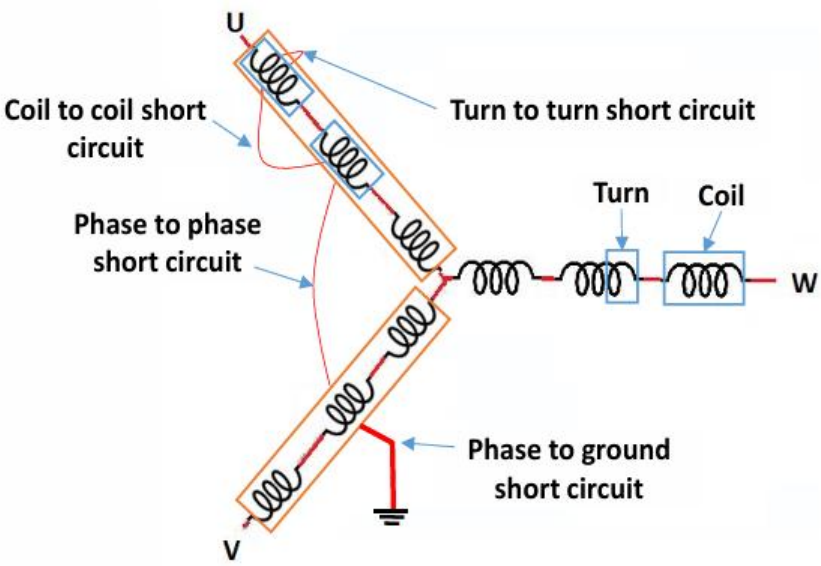

Figure 2.5 Stator Short-Circuit Faults in Induction Motors[9]

The coil-to-coil short circuit happens if the insulation between two adjacent coils in a winding fails, causing an imbalance in the winding and reduced efficiency.

The phase short circuit is caused by the failure of insulation between two phases. This results in a huge current flow that causes severe damage to the machine and plant. If a phase directly touches the frame ground of a machine or the grounding system of the plant, then a phase-to-ground fault occurs, which may trigger the protective relay or protective system to protect the plant from damage.

2.6 Causes and Effects of Inter-turn Fault

Electrical insulation is required in stator windings to prevent the conductors from short circuits. An inter-turn fault occurs when the insulation between stator conductors within the slot deteriorates, resulting in a short circuit. Due to the low impedance of this fault path, a large fault current can circulate through the affected windings, potentially causing severe localized damage. The causes of such short circuits can be mechanical, ambient, thermal, or electrical stress[11]. The thermal stress includes overheating from overloading or poor cooling, electrical stress is referred as voltage surges and transients, mechanical stress means vibration or movement that may cause insulation wear, and one of the causes of insulation degradation is manufacturing defects. The common reasons for stator core failures are[12]:

i. Excessive heating of the stator core or windings
ii. Improper installation or misalignment of end winding support systems
iii. Contamination of windings by dust, oil, moisture, or other pollutants
iv. Occurrence of short circuits within the winding
v. Mechanical and thermal stress due to high inrush currents
vi. Electrical discharges stemming from insulation degradation
vii. Malfunction or failure of the cooling mechanism

An increase in current density between the turns exceeding rated values is the main consequence of an inter-turn fault, creating a hot spot area around it. The insulation failure between turns of a stator includes a huge current flowing between the shorted turns, resulting in additional heat generation, which may destroy the adjacent turn, coil, or windings' insulation[13]. The initiation of an inter-turn fault in a machine is considered irreversible, as it can escalate into line-to-line or line-to-ground faults. Such faults may result in excessive current flow within the machine, potentially causing severe damage, posing significant fire risks and potentially causing system failure. That's why early detection of inter-turn faults is necessary.

2.7 Fault Detection Strategies for Stator Inter-turn Failures in IMs

Nowadays, IMs used in many industries are either fed by adjustable speed drives or by static power converters, which have PWM inverters as their operating element. For such machines, insulation breakdown is common due to frequent voltage spikes. Various techniques that have been utilized for the detection of stator inter-turn faults in IM till now. Some of them are briefly described below.

1. Motor Current Signature Analysis (MCSA) Technique

Detects faults by analyzing the frequency spectrum of the stator current, identifying characteristic frequency components related to specific faults. It involves examining the stator current through the Fast Fourier Transform (FFT) technique to detect characteristic frequency components associated with specific faults[14]. The principle of MCSA is to monitor the current flowing through the motor's stator and analyze its frequency spectrum to identify characteristic patterns that indicate a short circuit between adjacent turns within a phase. This method is not considered to be reliable in diagnosing the incipient faults. The MCSA is ineffective in the identification of stator turn faults as it cannot distinguish between faulty signals and other signals that may arise due to unbalanced voltage or harmonics injected due to adjustable speed drives.

2. Parks' Vector Approach

It is an approach used for the current monitoring of the machine. Three-phase current is converted into direct and quadrature (d-q) axes using this method. A motor's stator issue can be identified using the properties of both healthy and defective motors that have been removed[12]. It is a reliable approach to detect faults if the distortion caused by the fault is large, but fault detection in the initial stage is not very reliable through this method, as Park's vector approach depends on fault severity, noise level in the system, and loading condition of the machine.

3. Negative Sequence Current Analysis

Monitoring the negative sequence current allows for early detection of asymmetrical faults such as turn-to-turn short circuits. This technique is particularly useful in inverter-driven induction motors, where high-frequency switching can make conventional fault detection more challenging. These conditions can interfere with accurate fault detection, leading to potential misinterpretation of results[8].

4. Vibration Analysis

Online vibration monitoring is frequently applied to evaluate the bearing health of components. However, this method has certain limitations, particularly in identifying electrical malfunctions such as short-circuit conditions or internal mechanical issues within the machine itself[9].

5. Partial Discharge Measurement

To estimate the dielectric strength of the stator windings, PD measurements are utilized[15]. Online methods that use partial discharge detection and analysis work well for detecting short-circuited turn failures in big electrical machines. These techniques, however, are inappropriate for low-voltage devices, particularly those driven by variable speed drives.

6. Frequency Response Analysis

An established method for evaluating a power transformer's electrical and mechanical qualities is frequency response analysis, which is acknowledged globally[16]. The FRA approach provides a distinct signature for specific equipment or machines. When faults occur, they lead to alterations in the frequency response pattern[15]. The FRA method is renowned for its great sensitivity, which enables it to detect internal machine changes early on. Initial stator winding short circuits might not affect the machine's operation right away, but they can quickly worsen and cause serious harm. Thus, to stop more damage and guarantee dependable machine operation, early identification and prompt action are crucial[9]. Hence FRA technique is considered suitable for detecting the turn fault of the IM’s stator.

2.8 Frequency Response Analysis Technique

Insulation failure brought on by overloading, aging insulation, and mechanical vibrations can result in short-circuit problems in the stator windings of rotating machinery. Dielectric response analysis, when combined with FRA, can be an effective procedure for evaluating the state of stator windings and detecting defects. In the FRA technique, a voltage signal of low value with a broad frequency spectrum is introduced to one terminal of the winding, and the corresponding response is measured at the other terminal. High dynamic range, high accuracy, minimal test voltage requirements, improved sensitivity, and safety are just a few benefits of FRA. FRA has been used

historically to discover mechanical problems in transformer's winding displacement and short faults, but it has also shown promise in detecting induction motor failures[17].

The working principle of the FRA technique is to analyze the system's impedance or resonance characteristics over an applied frequency range. There are two fundamental methods to perform FRA on any machine: SFRA and IFRA. Both SFRA and IFRA are techniques used for evaluating machine condition. In SFRA, a low-voltage sinusoidal signal, frequency range that varies from Hz to MHz is introduced to one terminal of the machine, and the response is measured at the other terminal is measured or analyzed. In contrast, IFRA involves applying a high-frequency impulse signal and measuring the system's response. SFRA monitors condition changes over time through baseline comparisons, hence, it is commonly used for factory acceptance tests and post-fault diagnosis. On the other hand, IFRA is typically used in laboratories or controlled environments. Compared to IFRA, SFRA is less susceptible to interference, technically easier to implement, and provides higher precision across a broad frequency spectrum, making it a non-destructive method of condition monitoring[18]. SFRA requires a longer measurement time but provides high accuracy across the full frequency spectrum and provides an improved signal-to-noise ratio compared to IFRA[19].

The SFRA procedure is effective for detecting subtle changes in the windings caused by short circuits by analyzing the winding impedance across a broad frequency range. This method is extremely responsive to the inductive and capacitive coupling between winding turns, meaning any alteration in the winding's structure can significantly impact the frequency response. Insulation breakdown often begins with a turn-to-turn short circuit in a coil. Early detection of stator winding defects is crucial to stop the progression of insulation breakdown between the winding and the ground, which could result in ground fault currents and permanent damage to the stator core[6]. The methods to analyze the results may include:

(i) monitoring changes that have occurred in the frequency response curve
(ii) monitoring and comparing the formation of the creation of new resonant frequencies or the elimination of existing ones for different cases
(iii) monitoring and comparing significant shifts in the existing resonant frequencies

About one-third of all AC machine failures in industrial settings are caused by the stator insulation failure mechanism. These issues often start with a localized turn-to-turn breakdown. They are especially prevalent in adjustable speed drives (ASD) due to the turn-to-turn voltage, which can include spikes that cause partial discharge, leading to premature aging. For inverter-fed machines, assessing the condition of turn insulation becomes more difficult using traditional methods, which are typically the only means of detecting the earliest indications of insulation problems. As the turn insulation degrades due to aging, the resonance frequency also changes and capacitance increases with insulation aging[20].

An electric machine's overall impedance, which is influenced by its capacitances, winding resistance, self-, mutual, and leakage inductance, determines its frequency response[21]. The FRA approach is based on evaluating the equivalent impedance of the windings in the frequency domain. The frequency response of a stator winding is unique and can act as a "fingerprint" for the winding being tested, as it can be modeled as an equivalent circuit with a complex network of capacitances, resistances, and inductances. By comparing the observed frequency response to a reference response from a healthy winding, any deviations caused by physical or electrical changes to the winding can be detected[22].

The spectra can be compared chronologically (FRA measurements of the test object before deployment, also called fingerprint or reference spectra, and after a certain amount of operation), type-wise (FRA spectra of identical units, also called sister-units), and phase-wise (comparing the frequency responses of the various test object phases)[23]. Three primary methods exist to measure the frequency response or impedance of an electric machine: The direct tests for open-circuit and short-circuit conditions, along with the indirect testing method. During the direct short-circuit test, the stator winding is subjected to a short circuit, and a similar procedure is followed for the rotor in its respective test. In the indirect test, a voltage is applied to the field winding, and the resulting response from the stator winding is recorded, or vice versa. The direct open-circuit test involves applying voltage to one terminal of a winding and then measuring the response at the opposite terminal of the same winding[24].

2.9 High-Frequency Modeling of Stator

In many industries, induction motors fed by either adjustable speed drives or with static power converters having PWM as their operating components are commonly used. According to various works of literature, the modeling of induction motors can be done by including two branches in high-frequency operation, viz stator winding in the motor frame path and the stator winding turn-to-turn path refer to distinct electrical impedance paths within an induction motor. There are two categories of high-frequency machine models: An analogous circuit model based on finite element analysis (FEA) or numerical modeling, and behavioral equivalent circuit models [25]. 3-D electromagnetic field analysis involves simulating the motor's electromagnetic behavior in three dimensions, allowing for a more accurate representation of its performance[26]. The measurement based modeling method requires actual motor measurement data to develop an equivalent circuit that accurately reflects the motor's impedance. The behavioral method itself has two approaches: asymptotic and analytical.

Most of the work on machine modeling for electromagnetic interference (EMI) simulation has employed the behavioral modeling approach, as accurately reconstructing the motor’s 3-D structure from a known physical design remains a challenging task. This difficulty can lead to mistakes in impedance modeling that occur when utilizing finite element analysis[27]. In the behavioral approach, the induction motor can be modeled as a network with components of resistance, capacitance, and inductance. It has a unique frequency response in each operating condition. Any physical or electrical change in a winding component causes a shift in the response, which can be identified by comparing it to the fingerprint response. The response can be captured using an impedance analyzer or a frequency response analyzer[28]. Since the motor frame is often grounded, electromagnetic interference from both DM and CM must be taken into account[29].

To characterize high-frequency machine models, it is essential to measure the machine's DM and CM impedance in the range of tens of megahertz. To completely describe the electrical model representing a stator winding with any given connection configuration, impedance measurement only requires one stator winding configuration, and it becomes straightforward for frequency-based measurement as it is made possible through the resonant points observed in the measured data of impedance[25].

Due to high-frequency switching components of inverter-fed motor drives, undesired harmonic voltage components may arise, which cause high-frequency current to flow in the motor, affecting the insulation system in the stator winding. Because stray and parasitic motor characteristics are important at high frequencies, the current harmonics' route propagation is somewhat unexpected[29]. To detect extra resonant frequencies resulting from the influence of inter-turn capacitance, an R_T-L_T-C_T configuration is employed [30], [31].

The capacitance between the stator winding and the stator frame (C_{G1}+C_{G2}) influences the motor's response in the low-frequency range, specifically beneath the first antiresonance point. However, the capacitor C_{G1} plays a crucial role in the CM and DM impedance behavior at higher frequencies, above the first antiresonance. The Resistance R_G (R_{G1}+ R_{G2}) provides the resistance of the common-mode (CM) current path through the laminated iron core[32].

2.10 Statistical Analysis

The fault diagnosis using frequency response analysis or impedance analysis technique is a graphical method of fault detection. The fault diagnosis decision highly depends on the expert's opinion. The Correlation factor, total logarithmic error, standard deviation and mean squared error collectively serve as key statistical indicators for evaluating variations in frequency response characteristics computed for the healthy signature to measure the impact of such flaws[33].

FRA interpretation involves utilizing numerical indices to analyze and assess the frequency response data, which quantifies the variations in FRA traces and aids in making decisions regarding a machine's condition based on this quantified value[34]. For fault diagnosis, proper interpretation of FRA results is crucial[35]. Various statistical indicators are used, including correlation coefficient, sum of logarithmic error, standard deviation, absolute differences (DABS), mean square error, root of mean square error, covariance (COVAR), and minimum-maximum ratio (MM), among others., that are used to analyze the Frequency Response Analysis result[9].

The resonant frequency shift, its emergence or disappearance, and the variation in the amplitude differential between a functioning and malfunctioning TPIM can all be detected by CC[15]. The IEEE standard recommends that the CC calculate the variation between two frequency response signals, while ASLE is a highly responsive

statistical measure for identifying variations in frequency response, offering significant fault identification capability. SD increases with the severity of the short circuit (SC), while MSE amplifies errors caused by the squaring process in the equation[9]. Here, CC, ASLE, SD, and MSE are used. ASLE, SD, and MSE are likely better responsive than CC in detecting small alterations in the frequency response signature.

2.11 Significance of Calculation of These Statistical Indicators

(i) Improved Fault Detection

Frequency response signatures can exhibit small changes due to inter-turn faults, which may not be visually obvious. Statistical indicators such as CC and ASLE help to increase the sensitivity of fault detection.

(ii) Automation in Diagnosis

Numerical matrices enable automatic fault detection without manual inspection of frequency response analysis plots, providing the facility to be less human-intensive.

(iii) Comparative Study

Different fault levels and locations can be diagnosed by calculating and comparing different statistical indicators for different scenarios of the faults.

Chapter 3 Methodology

This chapter describes the method, tools, and techniques used, starting from data acquisition, high-frequency modeling of the machine, and validation of the machine for the detection of the stator turn-to-turn fault of an induction motor.

3.1 Approach

At first, the necessary literature review is done to understand the concepts, needs, and development of fault diagnosis techniques and condition monitoring. The required data is then collected from the experimental setup at the Tallinn University of Technology, Estonia. The signal analysis of data is done to evaluate the impedance response of the machines in both their operational and faulty states. The overall methodology used in this research work is shown in Figure 3.1 below:

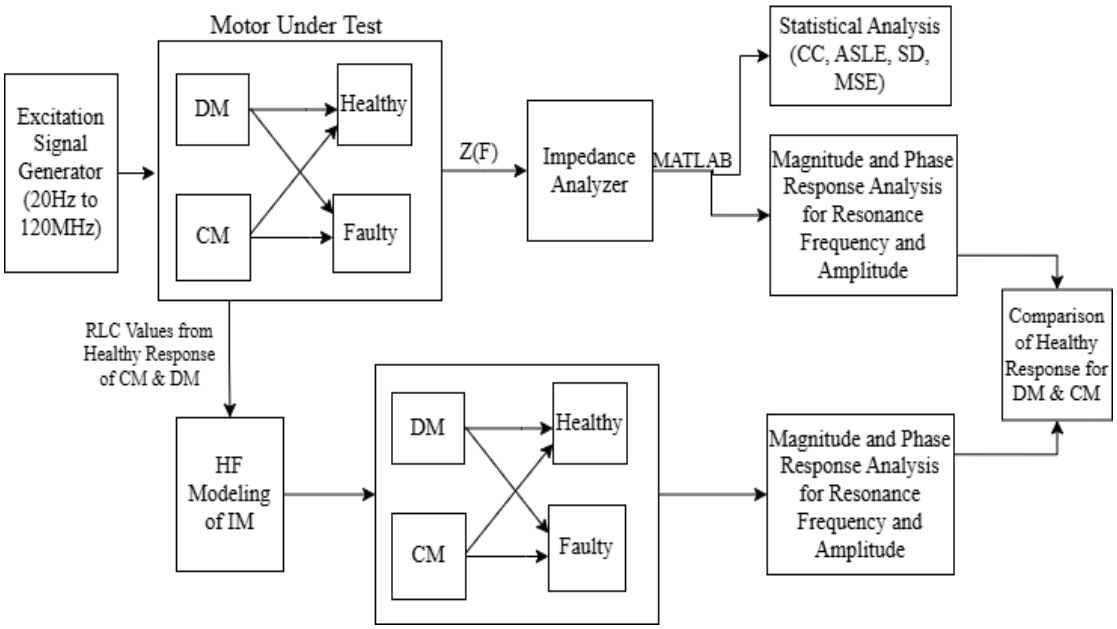

Figure 3.1 Flow diagram of the approach

3.2 Tools and Software

Advancements in computer architecture, software, and programming tools have significantly simplified the modeling and analysis of power systems. In earlier times, these tasks were often challenging, time-consuming, and prone to inaccuracies due to the limited capabilities of processing tools and outdated software. In this section, the tools used to carry out this dissertation are listed.

3.2.1 Microsoft Office

Microsoft Office, or MS Office is a productivity suite created by Microsoft that includes applications such as Word, Excel, and PowerPoint as the core products. In this study, Microsoft Word is used as documentation of the task, and Microsoft Excel is used to store the experimental data.

3.2.2 MATLAB

MATLAB, short for Matrix Laboratory, is a proprietary software application that supports multi-framework programming languages and numerical computing environment constructed by MathWorks. It provides powerful tools for matrix operations, data visualization, algorithm development, user interface design, and integration with applications written in other programming languages. In this work, MATLAB is used for the simulation of the model and signal processing of experimental data.

3.2.3 Diagrams.net

It is also known as draw.io. This tool is a free, open-source diagramming tool that helps to create different kinds of flow charts, electrical circuit diagrams, network diagrams, and many more. This online tool is used to draw different types of block diagrams and circuit diagrams.

3.3 Machine Impedances in a Frequency Sweep for Different Connections of Stator

Modeling electric machines for high-frequency operation requires consideration of both CM and DM impedances. The CM operation is obtained by connecting the supply between the common point of three phases and neutral, and the differential-mode operation is obtained by connecting the supply between a common point of two phases and the third phase. Both the differential and common modes can be understood in Figure 3.2. In Differential Mode (DM) measurements, the impedance obtained represents the overall differential-mode impedance experienced by the phase currents as a whole, rather than the individual impedance corresponding to a single phase in the three-phase equivalent network. According to the literature review done so far, the increase in capacitance due to insulation degradation is regarded as a surrogate measure of dielectric wear, and its variations in this impedance can serve as an indicator of insulation aging between winding turns.

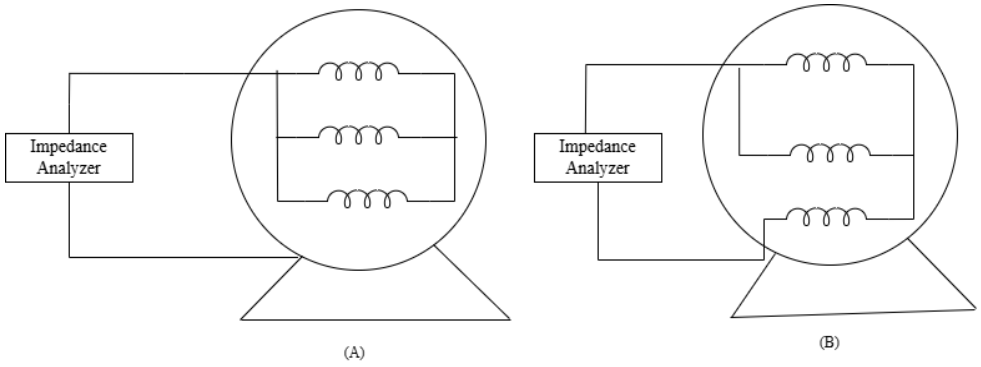

Figure 3.2 (A)Common mode connection and (B)Differential mode connection

Hence, the fault was created using a capacitor with variable capacitance. This is linked in parallel with the full winding. The circuit diagram illustrating this process is shown in Figure 3.3.

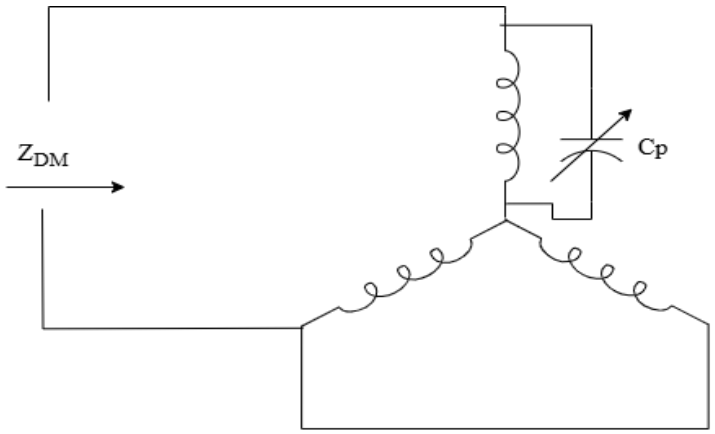

Figure 3.3 Inter-turn fault creation in the stator

3.4 Development of a High-Frequency Model for the IM

Characterizing high-frequency machine models involves measuring both differential and common-mode impedance across a wide frequency range, often up to several tens of megahertz. Notably, a single stator winding configuration is sufficient to perform these impedance measurements, enabling full modeling of the machine for arbitrary stator winding arrangements. The parameters used in Figure 3.4 have a significant meaning. The parameters are described as:

- ✓ R_G and C_G refer to the parasitic resistance and capacitance that exist between the stator winding and the motor casing, which are divided into R_{G1} and R_{G2} and C_{G1} and C_{G2} as phase-to-earth and neutral-to-earth capacitance and resistance

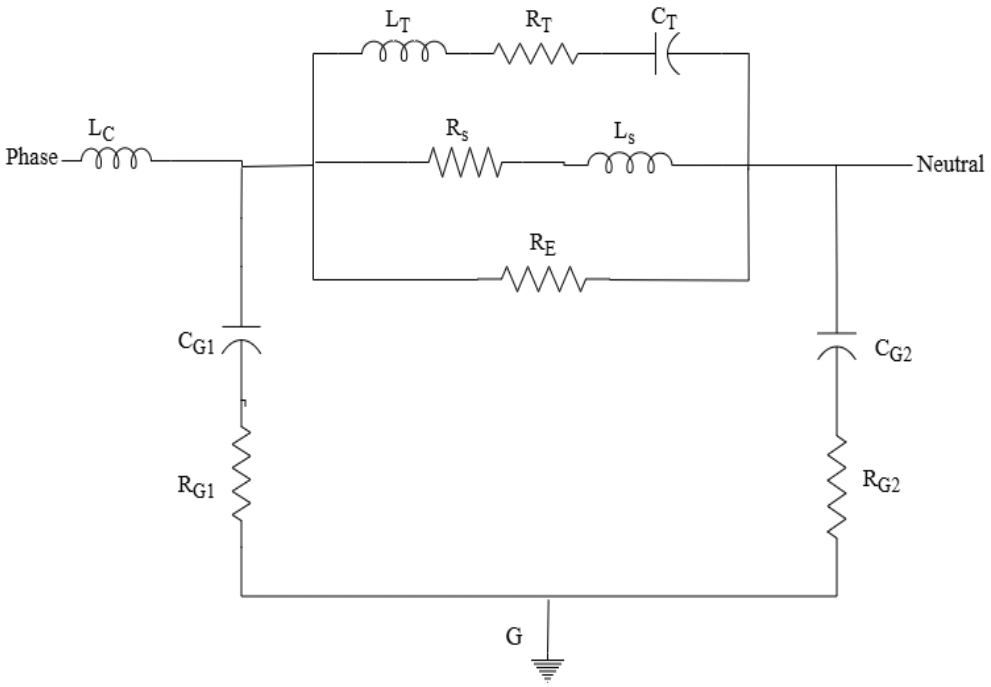

Figure 3.4 High-frequency model of the machine

respectively.

- ✓ L_S denotes the leakage inductance associated with the stator winding
- ✓ R_E is the high-frequency losses due to eddy currents in the stator core
- ✓ L_C represents the total inductance of the machine's internal feed conductors to the stator winding
- ✓ R_T, L_T, and C_T represent the second resonance observed in the motor's frequency characteristics, which could arise from the inter-turn capacitance effect of stator windings and the skin effect

The following relations are used to calculate the optimal values of parameters from the parallel and series resonance points shown as 1-4, and other values from the graph shown in Figure 3.5. The graph is the fingerprint of the machine for sweep frequency response analysis.

C_{TOTAL} and C_{HF} are calculated from the common-mode magnitude response, where the slope of the curve is -20dB/decade.

$$C_{G1} = \frac{1}{3} C_{HF} \qquad (3.1)$$

$$C_{G2} = \frac{1}{3}(C_{TOTAL}\text{-}C_{HF}) \quad (3.2)$$

Resonant-3 is the differential mode resonance frequency where the impedance has a minimum value.

$$R_{G1} = \frac{2}{3} Z_3 \quad (3.3)$$

Resonant-1 is the initial series resonance point of the CM response, where Z_1 is the corresponding impedance of the first resonance point.

$$R_{G2} = 3Z_1 \quad (3.4)$$

$$L_{CM} = \frac{1}{3} * \left(\frac{1}{2*\Pi*CG2*F1}\right)^2 \quad (3.5)$$

$$L_{DM} = \frac{ZL}{2*\Pi*Fl} \quad (3.6)$$

$$Ls = L_{CM} + \frac{4}{9} L_{DM} \quad (3.7)$$

Where L_{CM} is calculated from the resonance point-1, and L_{DM} is calculated from the response of the DM connection of the motor, where the slope of the response is +20dB/decade.

The resonant-4 point is the first parallel resonance point in the differential mode response of the test machine, which represents the maximum impedance.

$$R_E = \frac{2}{3} Z_4 \quad (3.8)$$

The resonant-2 is the second resonance point or the first resonance point in the differential mode response of the machine under test.

$$C_T = \frac{1}{10}(C_{G1} + C_{G2}) \quad (3.9)$$

$$L_T = \frac{1}{CT} * \left(\frac{1}{2*\Pi*F2}\right)^2 \quad (3.10)$$

$$R_T = Z_2 \quad (3.11)$$

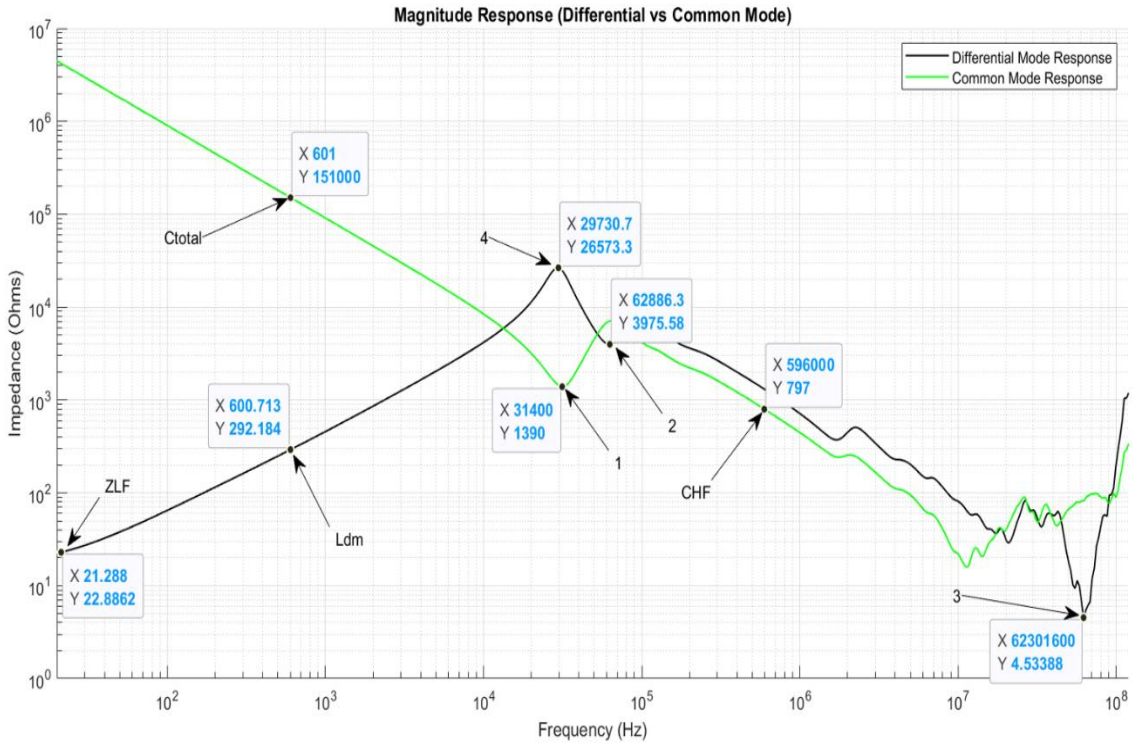

Figure 3.5 Measurement of impedance magnitude and key parameters of CM and DM for motor characterization in high frequency

where Z_2 is the impedance of resonant point 2, and L_C is determined from the resonant points 1 and 3.

$$L_C = \frac{1}{4*Cg1*f3\text{^}2} \qquad (3.12)$$

R_S is obtained from the initial point of the response in differential mode.

$$R_S = \frac{1}{2} Z_{LF}*\cos(\theta_{LF}) \qquad (3.13)$$

3.5 Statistical Indicators Being Calculated and Analyzed

3.5.1 Correlation Coefficient

The Correlation Coefficient (CC) is used to quantify the difference between two FRA responses, denoted as H(i) and F(i), as defined in equation (1). A CC value of 1 indicates that the two responses are identical, while values between 0 and 1 reflect the degree of similarity, with lower values indicating less correlation between the signals. This indicator is calculated from Equation (3.14).

$$CC(H,F) = \frac{\sum_{i=1}^{N} H(i)*F(i)}{\sum_{1}^{N} \sqrt{[H(i)]^2 * [F(i)]^2}} \quad (3.14)$$

3.5.2 Absolute Sum of Logarithmic Error

The average total of logarithmic errors normalizes data across different magnitudes, whether small or large, ensuring consistent comparison. It is computed using Equation (3.15).

$$ASLE(H,F) = \frac{\sum_{i=1}^{N} |20logF(i) - 20logH(i)|}{N} \quad (3.15)$$

3.5.3 Standard Deviation

The SD, given by Equation (3.16) can detect changes in two FRA responses and mirrors the trend of ASLE.

$$SD(H,F) = \sqrt{\frac{\sum_{i=1}^{N} [F(i) - H(i)]^2}{N-1}} \quad (3.16)$$

3.5.4 Mean Squared Error

The average squared error is highly sensitive to large deviations but less responsive to minor differences below one. It is computed as shown in Equation (3.17)

$$MSE(H,F) = \frac{\sum_{i=1}^{N} [F(i) - H(i)]^2}{N} \quad (3.17)$$

Where H and F represent the healthy and faulty responses, respectively, of the motor under test.

3.6 Experimental Work and Data Acquisition

The input of a signal generator, which can produce a signal of 20Hz to 120MHz, is fed to one terminal of the IM being tested, and the resulting response is detected through an impedance analyzer. The technical specifications of the induction motor used for the experiment are provided in Table 1, from the Department of Electrical Power and Mechatronics Engineering at Tallinn University of Technology, Estonia.

Table 3.1 *Induction Motor Parameters for the Study*

Induction Motor Specifications	**Parameters**	**Units**	**Value**
	Number of Phases		3

	Connection		Star
	Voltage	V	400
	Current	A	1.7
	Power	kW	0.75
	Speed	rpm	1440
	Power Factor		0.76

Figure 3.6 Showing the specifications/ nameplate of the induction motor used

Figure 3.7 E4990A Impedance Analyzer

The Keysight E4990A impedance analyzer is shown in Figure 3.7. The Keysight E4990A Impedance Analyzer is a high-precision instrument with an impedance measurement accuracy of 0.045%. It is designed to measure impedance characteristics across a broad frequency range that ranges from 20Hz up to 10, 20, 30, 50, or 120MHz.

It is widely used in research and development projects, quality assurance, and production factories as it can be applied to analyze passive elements such as capacitors, inductors, resistors, semiconductors, transformers, and motors. It has a DC bias source of ±40V/±100mA which is crucial for assessing semiconductor devices and materials that require controlled bias conditions. It has a built-in SSD to store data and supports multiple connectivity options such as USB, LAN, etc. The impedance analyzer can measure parameters such as |Z|, |Y|, θ, R, X, G, B, L, C, D, Q, Complex Z, Complex Y, V_{ac}, I_{ac}, V_{dc}, and I_{dc}. Table 2 contains the specifications of the impedance analyzer used.

Table 3.2 *Specifications of the Impedance Analyzer Used*

	Parameters	**Units**	**Values**
Impedance Analyzer Specifications	Frequency Range	Hz	$20\text{-}120*10^{6}$
	Impedance	Ω	$25*10^{-3}\text{-}40*10^{6}$
	Voltage	V	±40

First, the data for healthy conditions were obtained for the frequency range of 20Hz to 120MHz by connecting the motor in differential and common mode, as characterization of IM in high-frequency operation requires differential and common mode data. The connection diagram for DM and CM is given in Figure 3.2. A fault was created using various values of capacitors, which were connected in parallel to a whole winding, as various literature states that as the insulation degradation occurs, the capacitance of the insulating material increases due to the reduction in dielectric property of the material. The signal analysis of the obtained data was done in MATLAB software.

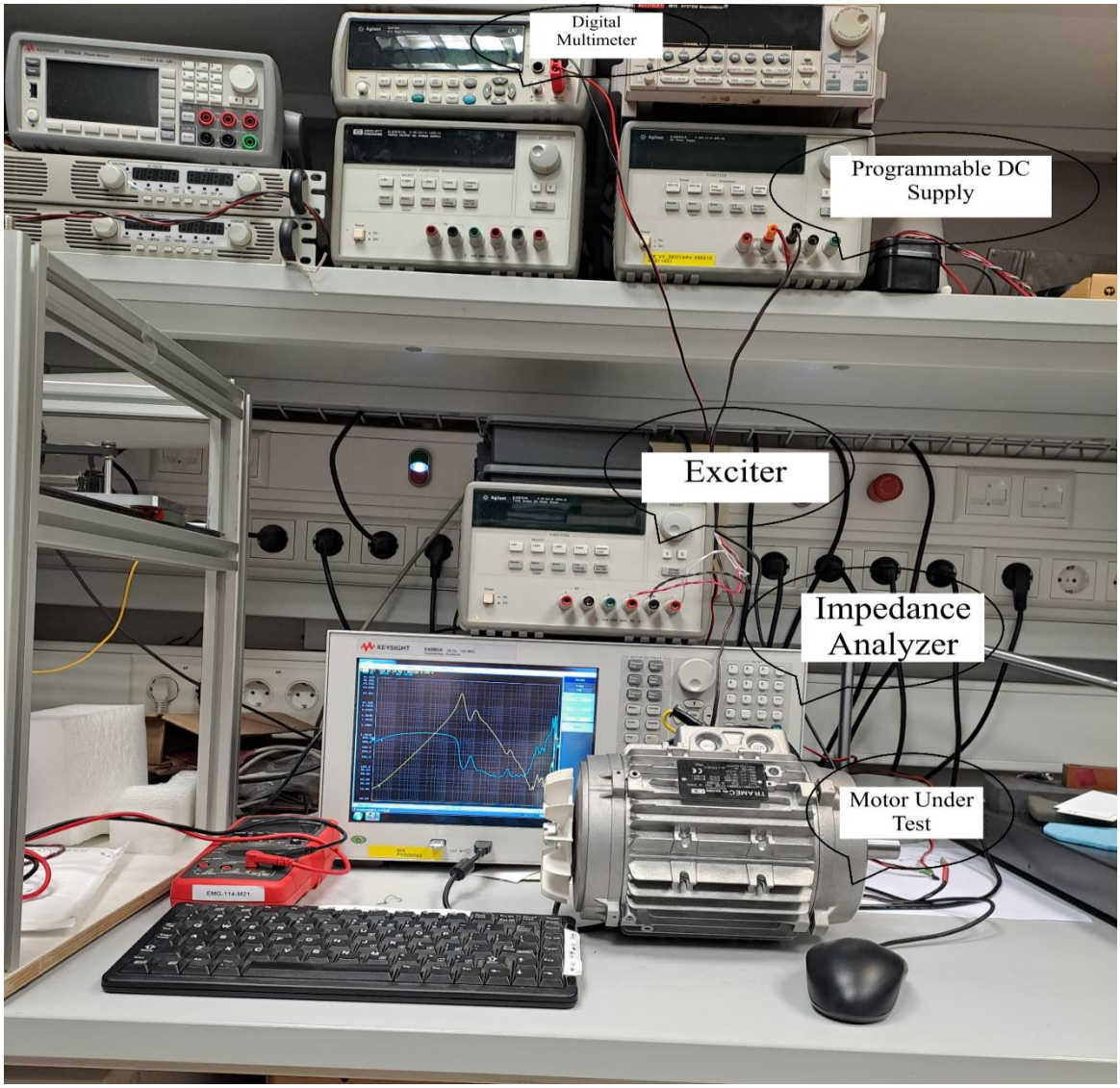

Figure 3.8 Experimental setup to get the data for FRA

Chapter 4 Results and Discussion

The results from experimental tests, model simulations, and statistical analysis of the star-connected stator winding of the induction motor are discussed in this chapter.

4.1 Simulation Results of the HF Model by Connecting in CM and DM modes as shown in Appendix B

The responses obtained from the simulation of the per-phase model shown in Figure 3.4 for different cases are shown in Figures 4.1, 4.2, 4.3, 4.4, 4.5, and 4.6. Figures 4.1 and 4.2 are obtained by simulating the model using the optimal values shown in Appendix A, which show magnitude and phase responses under normal operating conditions of the machine. These can be used as references for other simulation results. Figures 4.3-4.6 are obtained by connecting the per-phase model shown in Figure 3.4 in differential mode and common mode connection, respectively. These results show faults that are characterized by decreased impedance magnitude and resonance at lower frequencies as the variation in capacitance occurs.

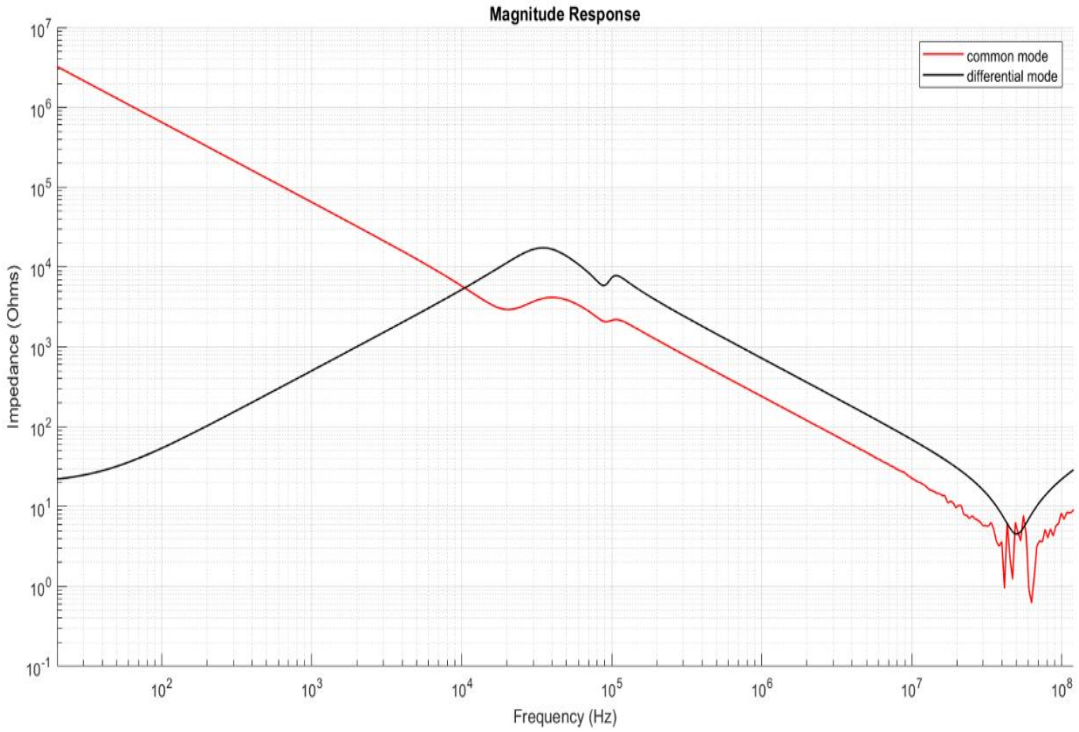

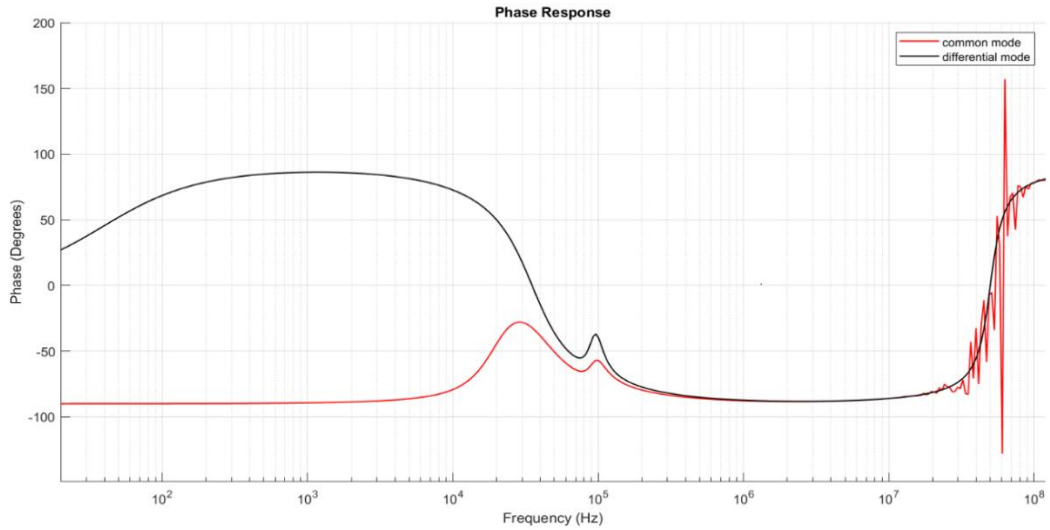

Figure 4.1 Magnitude and phase behavior of the CM and DM connection

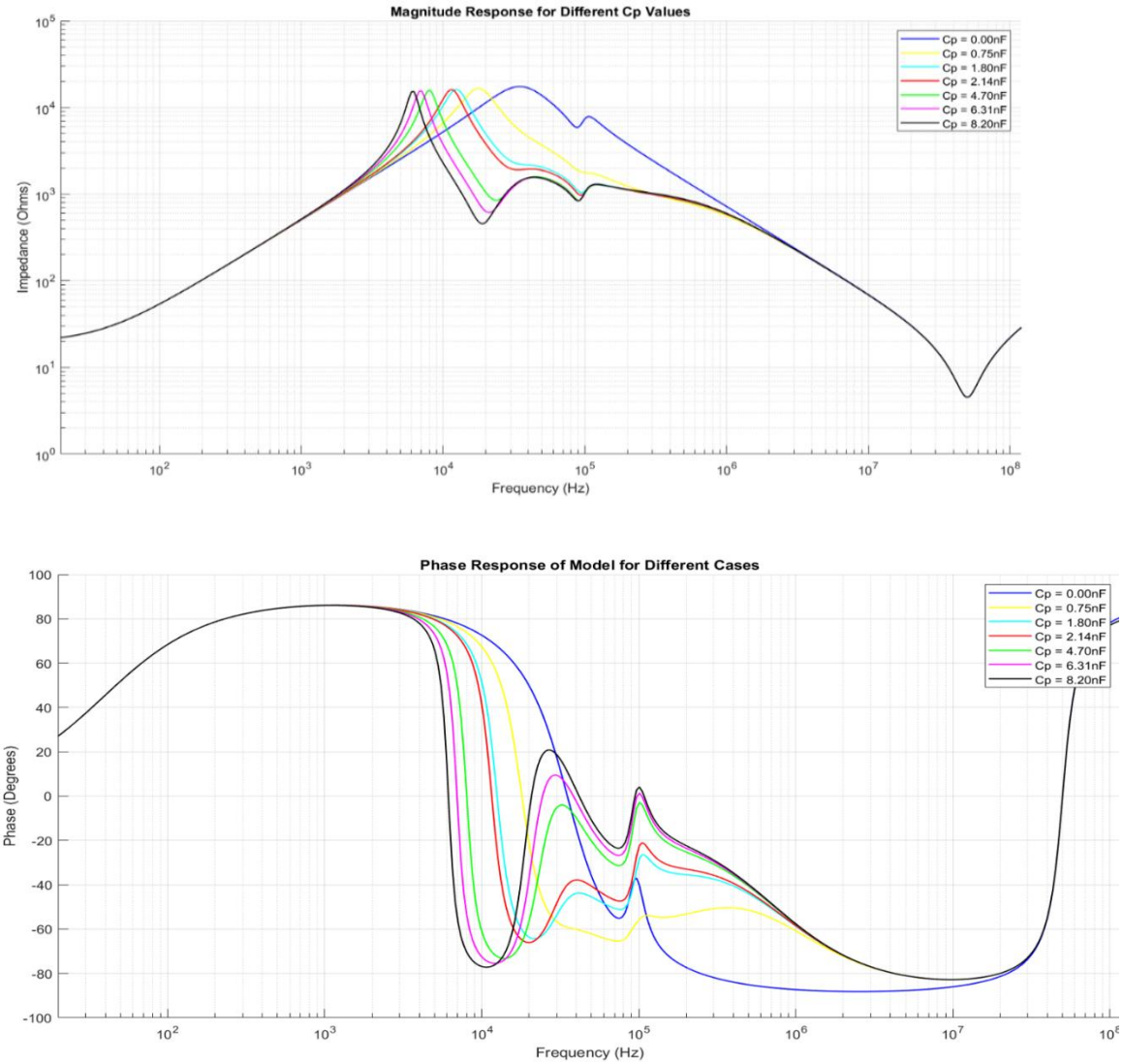

Figure 4.2 Magnitude and phase behavior of the model for variable Cp values in DM

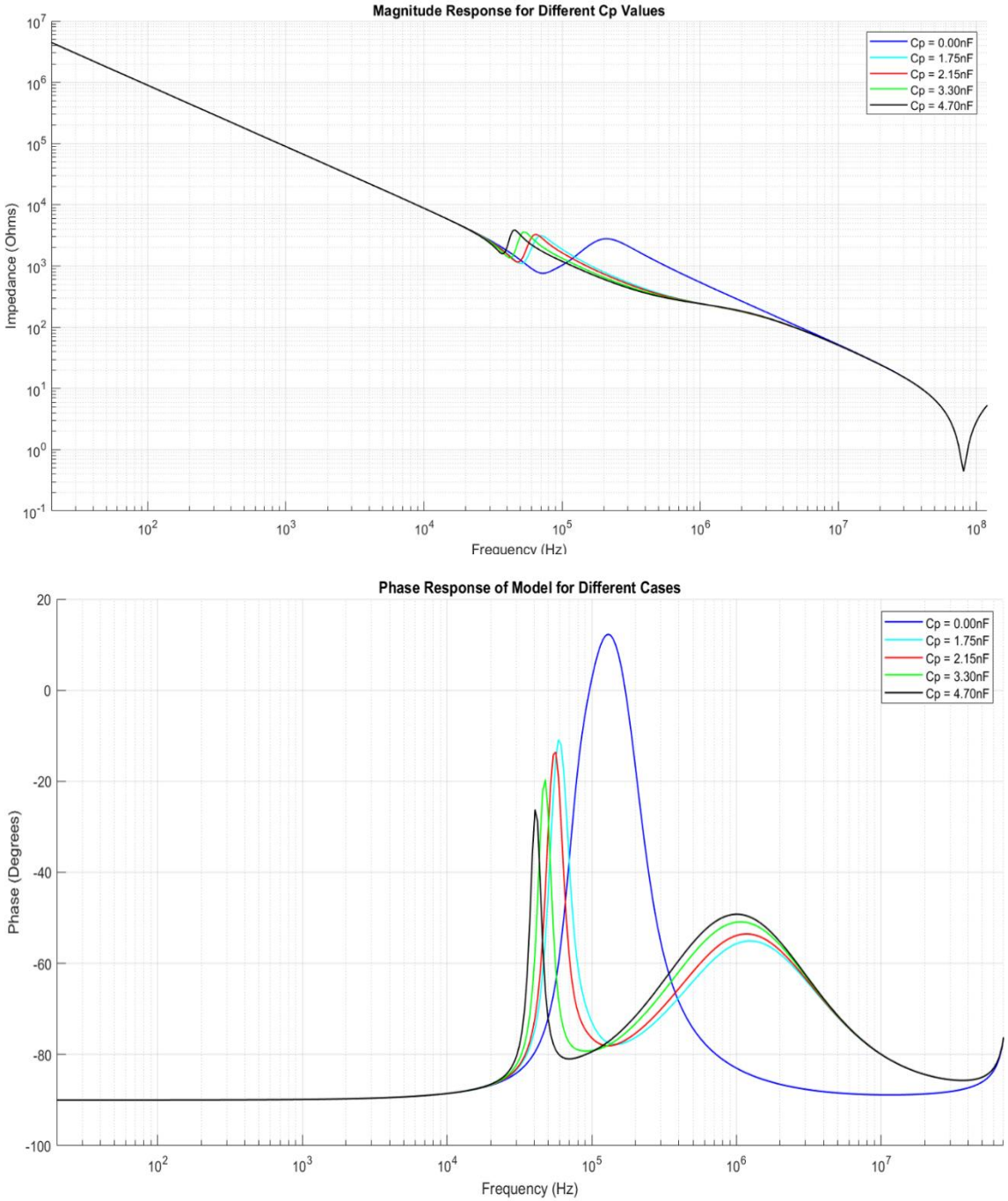

Figure 4.3 Magnitude and phase behavior of the model in CM for different capacitors

4.2 Results Obtained from the Signal Analysis of Experimental Data

Figure 4.7 depicts the response obtained from the motor while it is in normal operating condition and it can be used as the fingerprint response to compare the results obtained for various operating conditions.

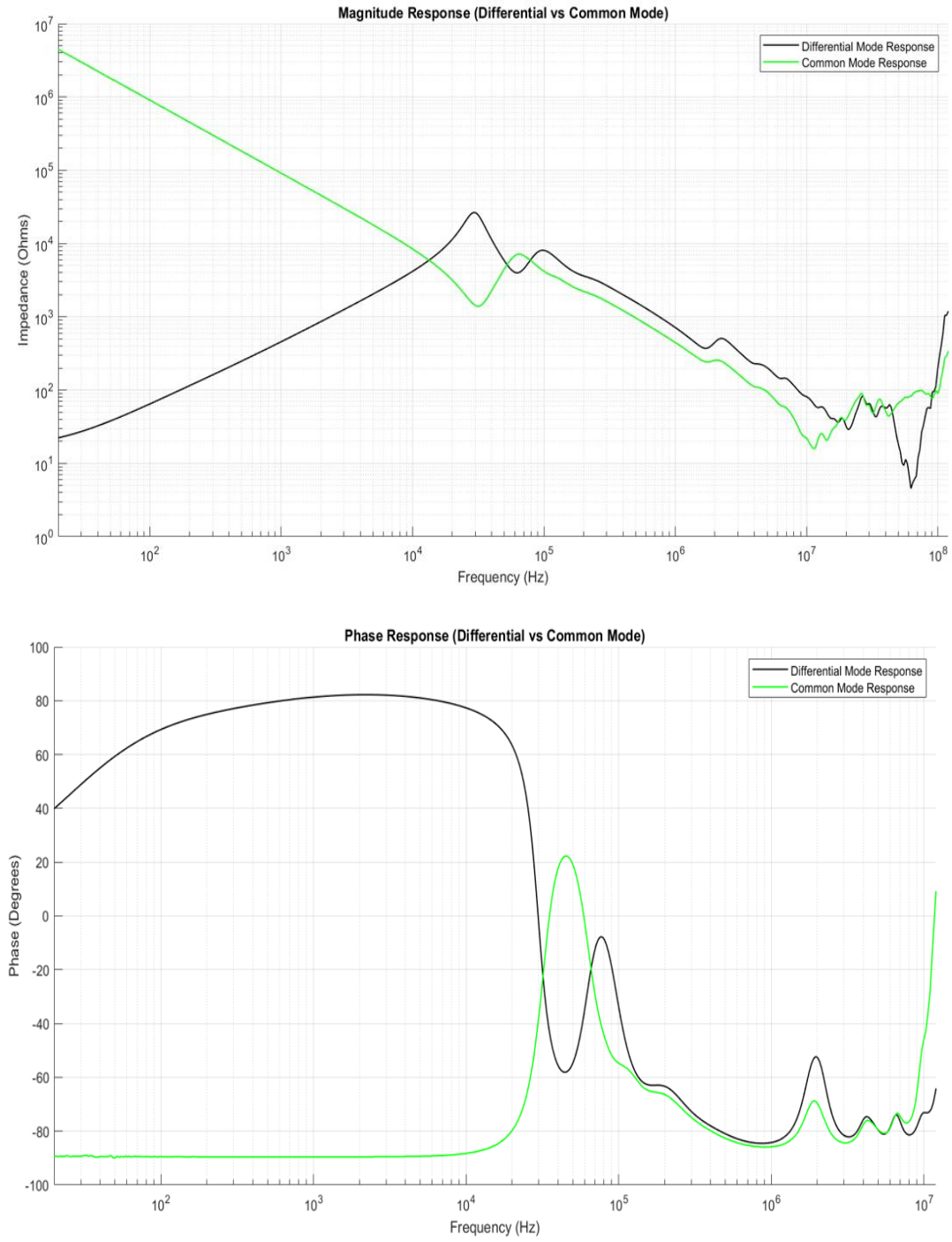

Figure 4.4 Magnitude and phase characteristics of differential and common modes connection under normal operating conditions of motor

From Figures 4.8 and 4.9, it is seen that the response shifts to the left in the event of insulation degradation between turns, indicating a reduction in the effective inductance caused by inter-turn faults. This shift strongly shows that the electrical circuit parameters are changed due to short circuits in the winding. In degraded response, resonance peaks are less pronounced, suggesting increased energy dissipation due to circulating currents that are generated due to inter-turn fault. This might be a case of low impedance path which is a characteristic of inter-turn fault.

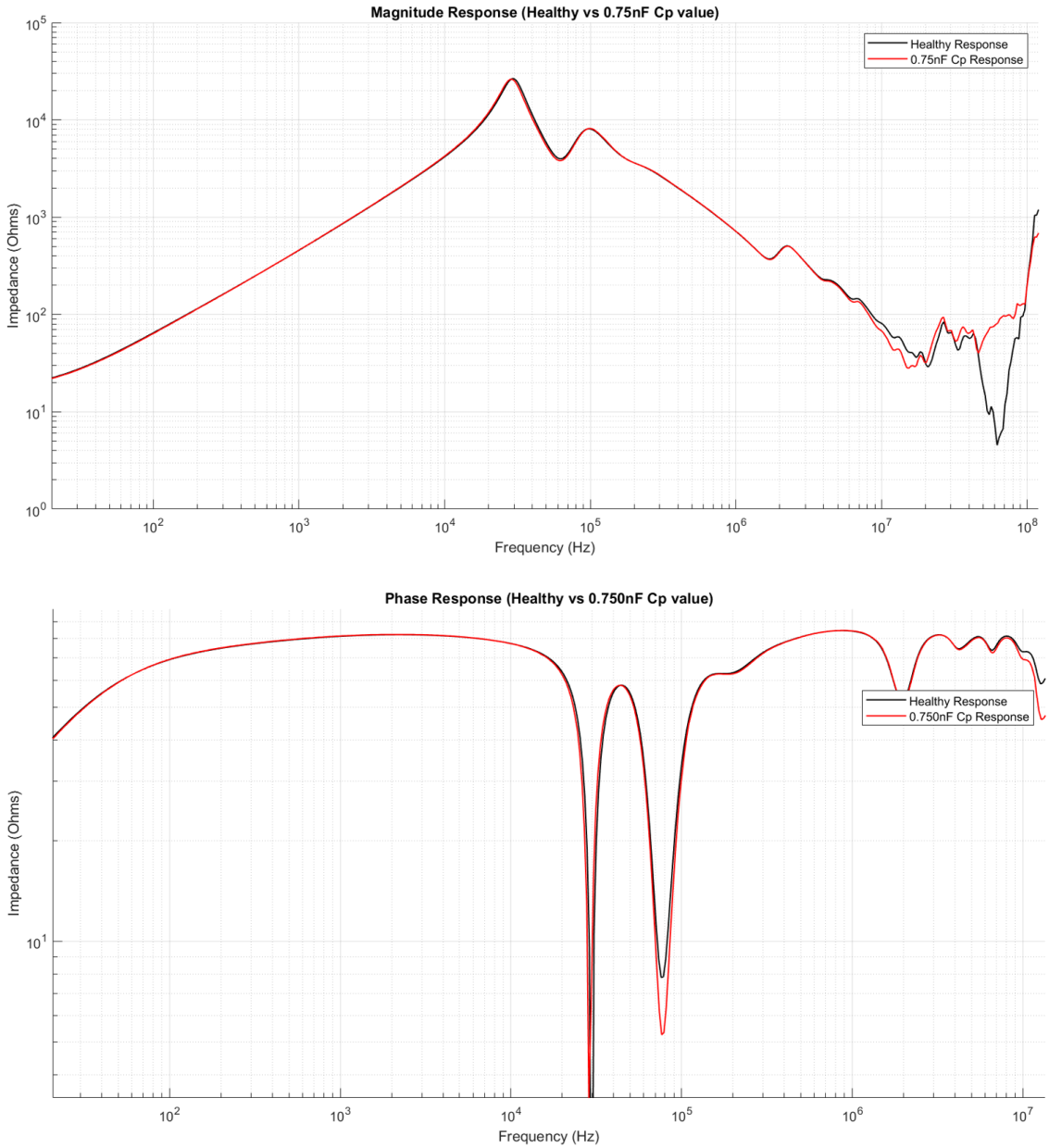

Figure 4.5 Comparison of response obtained by connecting a capacitor of 0.75nF in parallel with a phase to normal condition

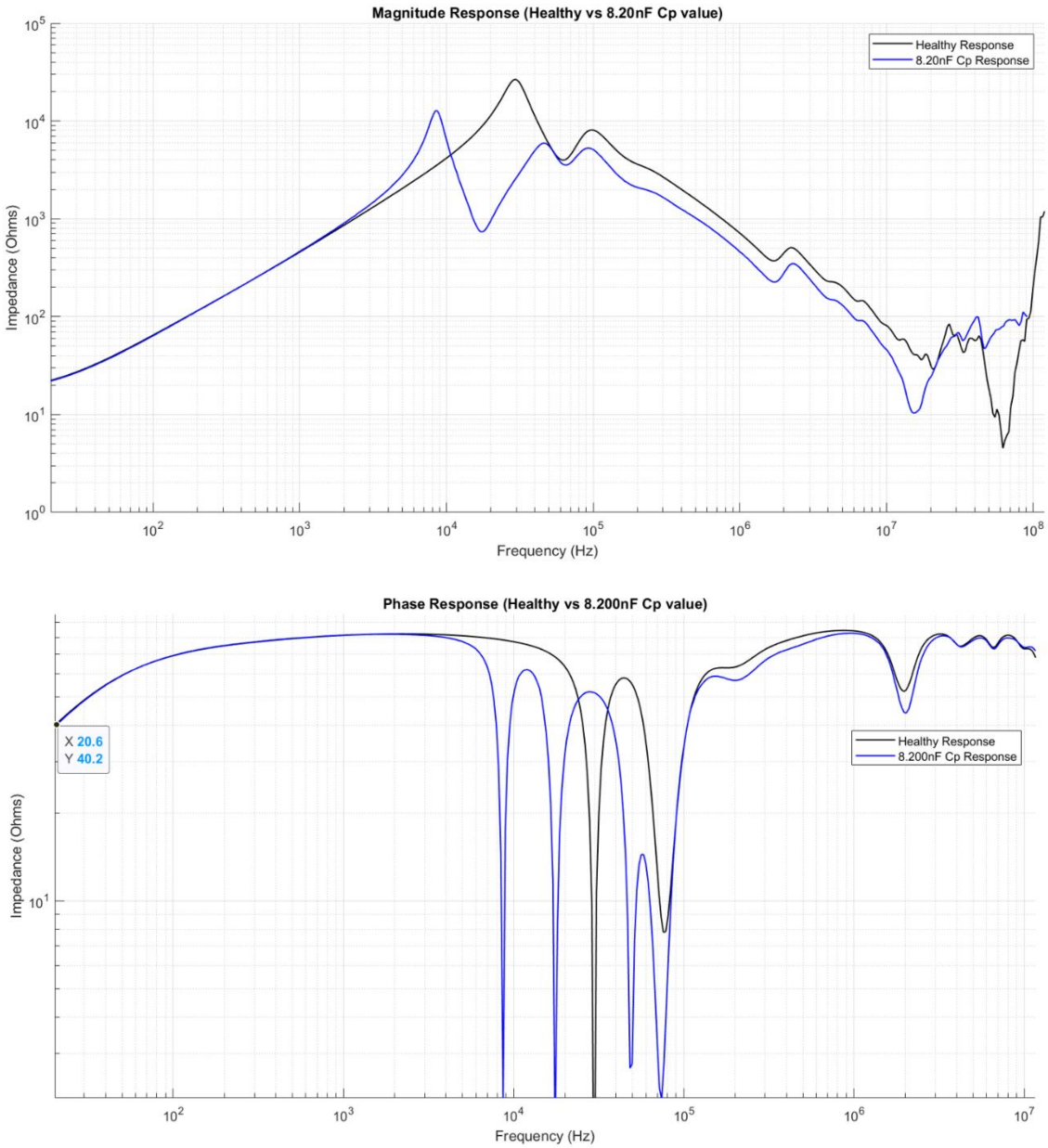

Figure 4.6 Comparison of response obtained by connecting a capacitor of 8.20nF in parallel with a phase to normal condition

From Figures 4.10 and 4.11, we can observe that the magnitude response shows a deviation that confirms changes in the electrical parameters of the stator. At higher frequencies, the fluctuation of the response of the degraded cases shows an increase in parasitic capacitance and leakage currents in the faulty winding. The phase response shows a phase lead at lower frequencies, indicating altered inductance, which points to an imbalance in the mutual coupling of winding conforming to the manifestation of a turn fault. The unstable phase response beyond the frequency of 10^7 Hz shows a localized insulation failure that could progress to more severe damage.

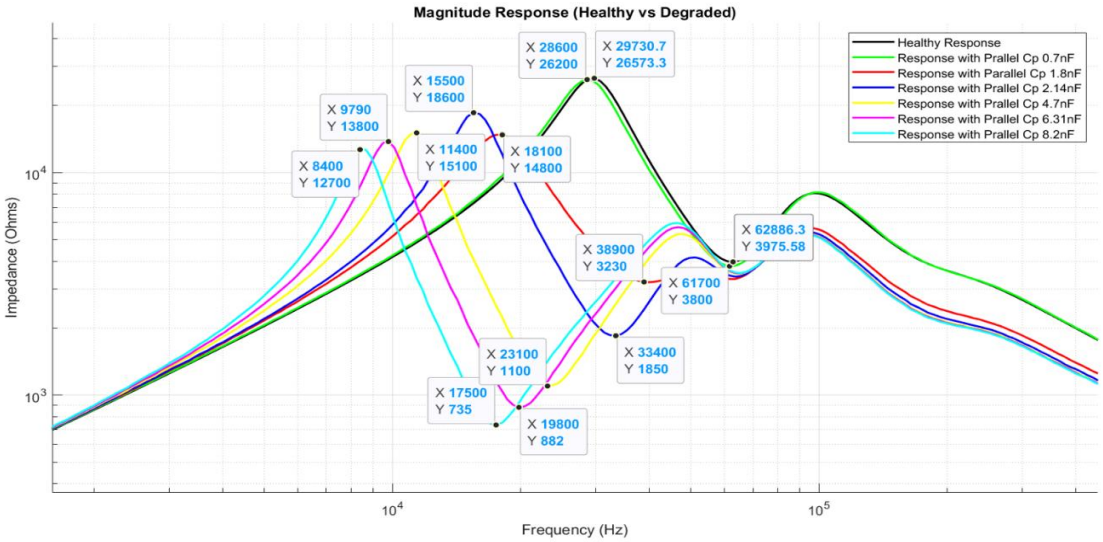

Figure 4.7 Zoomed magnitude response showing the first parallel and series resonance

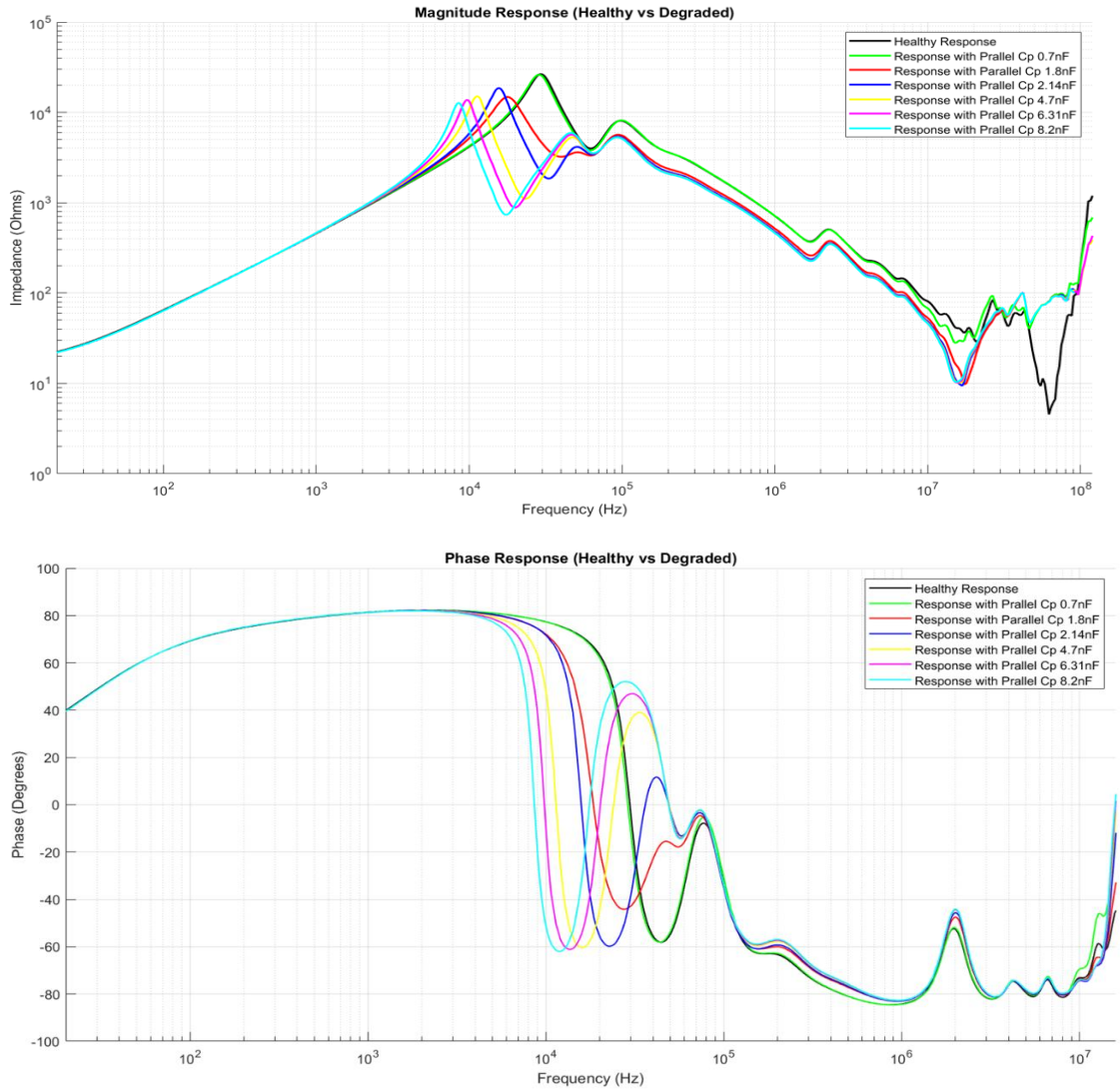

Figure 4.8 Magnitude and phase response of normal and various cases of insulation degradation

In Figure 4.12, it is seen that the common mode connection has almost the same magnitude and phase response for various operating conditions. Thus, from visual inspection, it is seen that the common mode connection is not better for detecting inter-turn faults caused by insulation degradation. However, this scenario is not supported by statistical analysis.

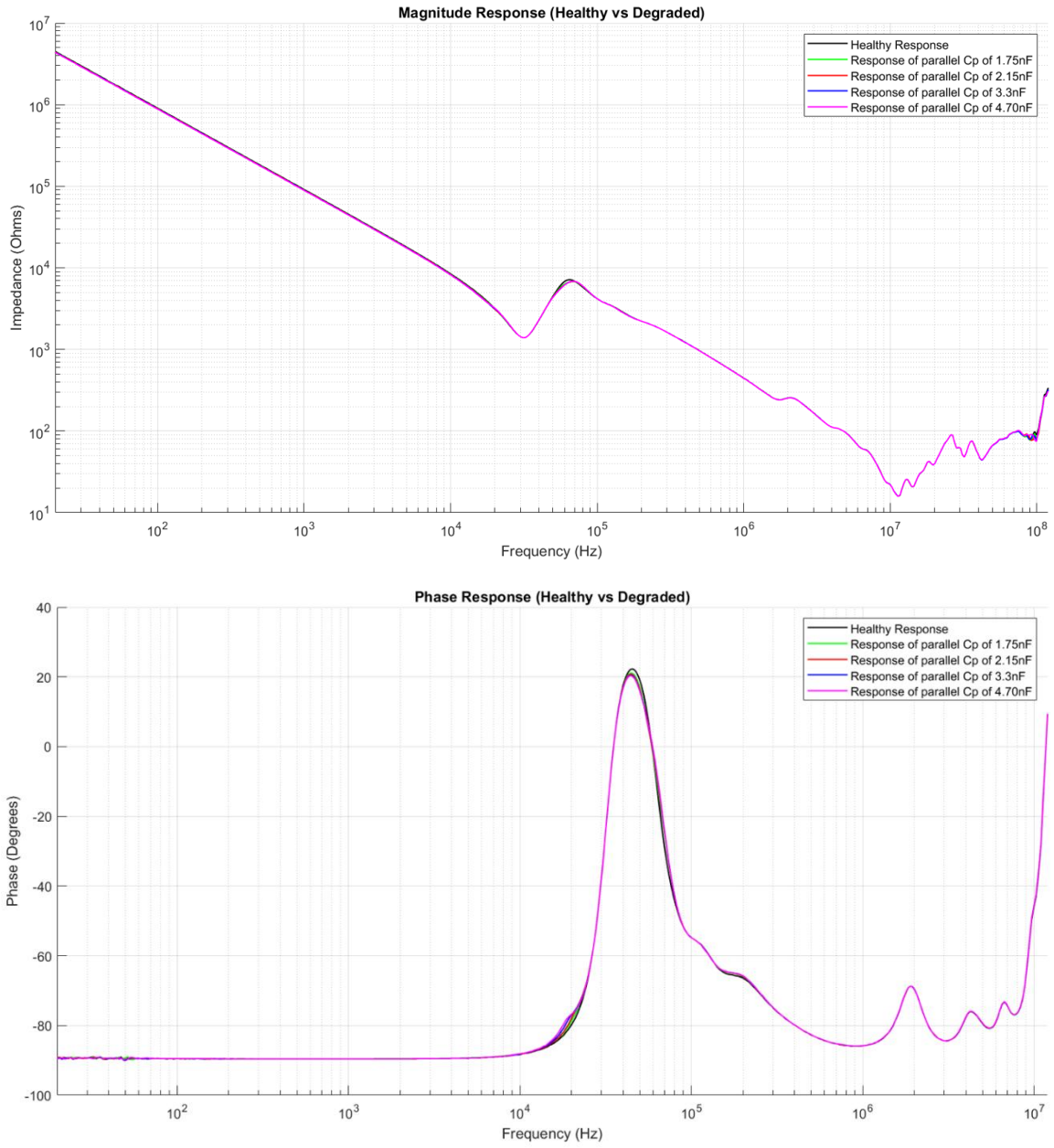

Figure 4.9 Magnitude and phase response of different cases of common-mode connection

4.3 Experimental Verification of the Per-Phase Model for Inter-Turn Fault Detection

The model's magnitude response indicates that it agrees with the motor's experimental sweep frequency response. Figures 4.13 and 4.14 demonstrate that the established per-phase model can accurately emulate a short circuit between turns in the stator winding, hence validating the suggested model.

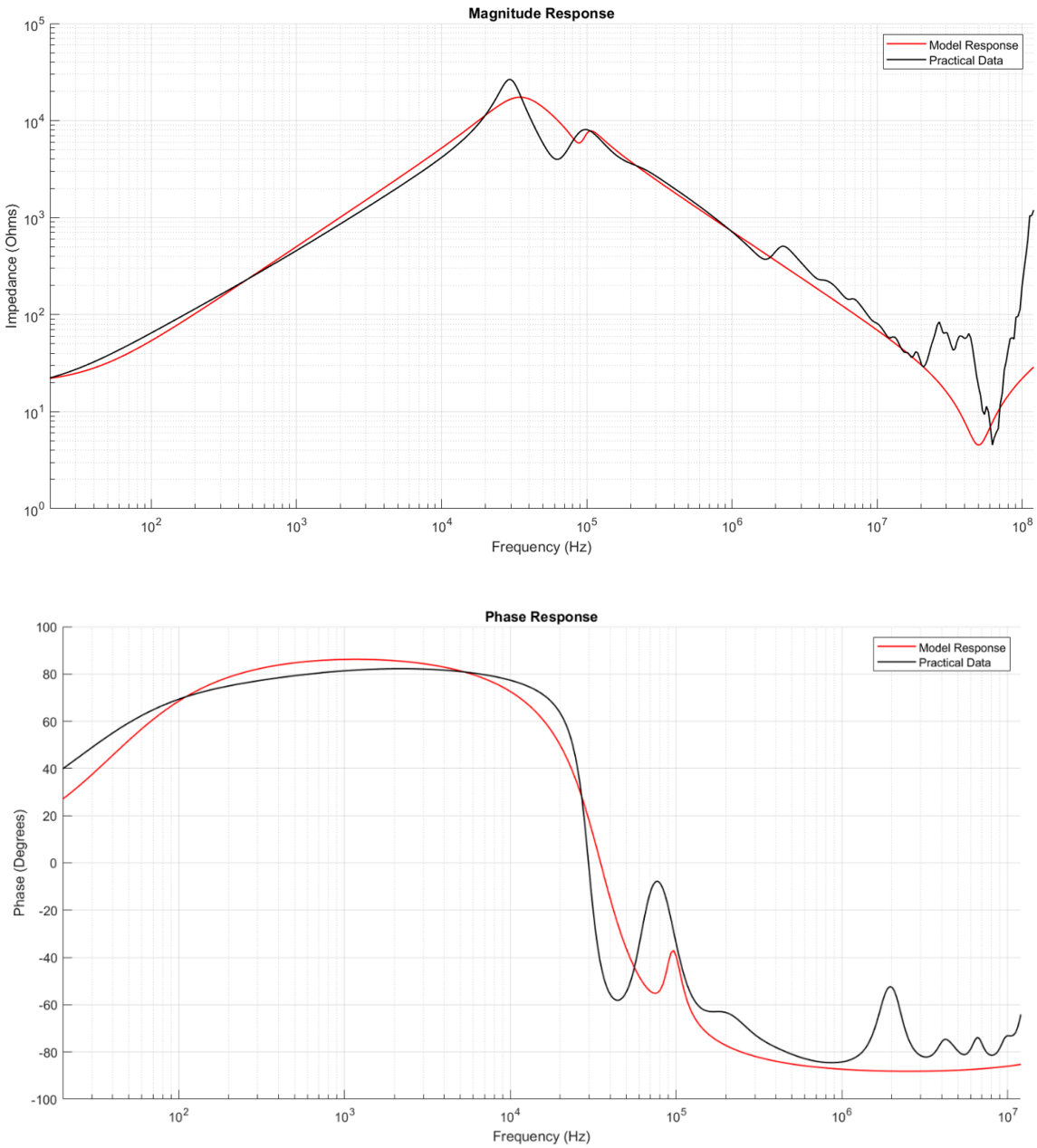

Figure 4.10 Comparison between the model response and the experimental results in the differential mode of connection under normal operating conditions

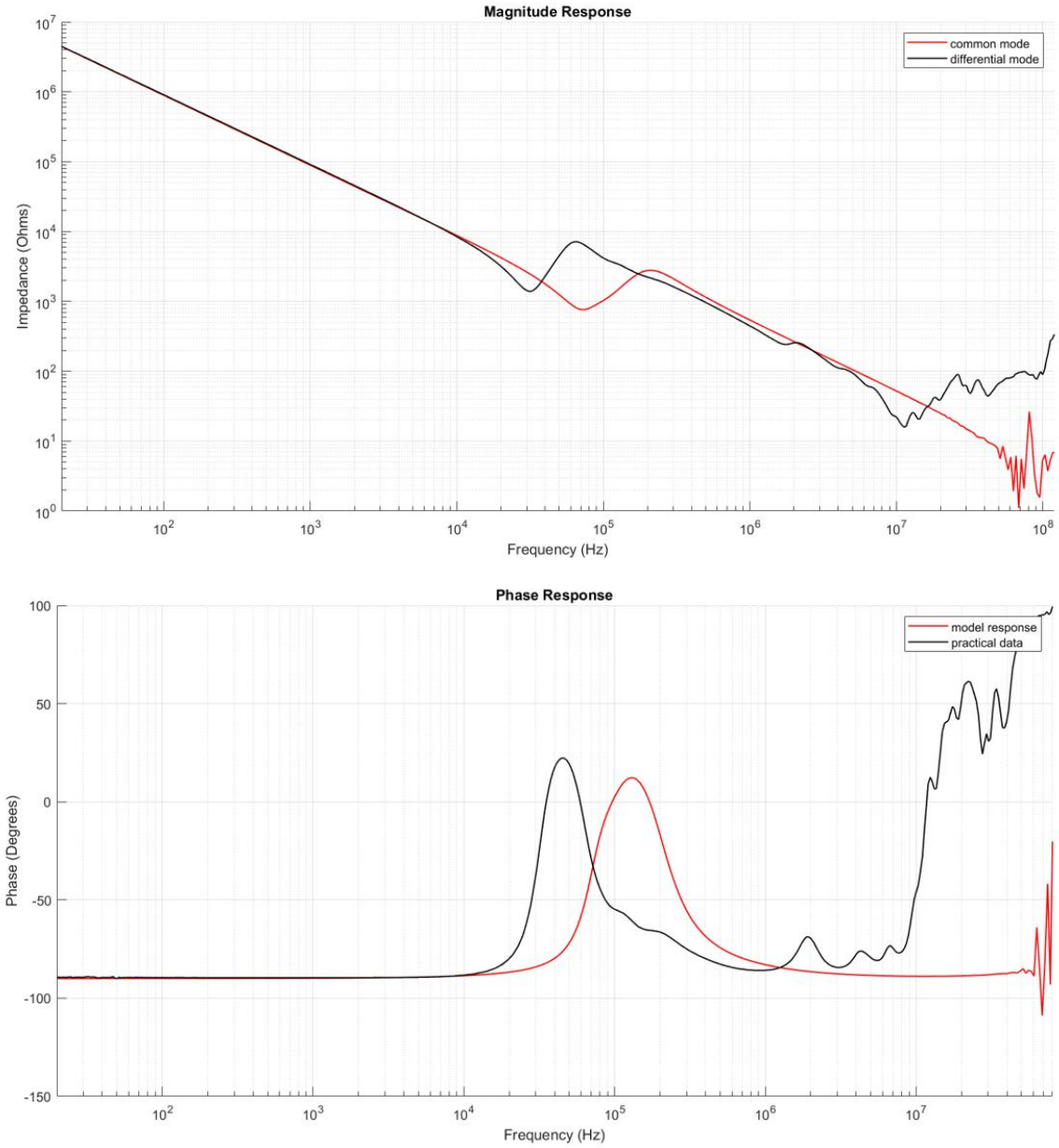

Figure 4.11 Response of the model compared to the experimental response in common mode of connection under normal operating conditions

4.4 Results of Statistical Analysis of the Response

For the calculation of different statistical indicators, the whole frequency band (20Hz to 120MHz) is divided into three frequency bands to make the decision-making process more effective. Those frequency bands include the low-frequency band (20Hz to 1kHz), medium-frequency band (1kHz to 1MHz), and high-frequency band (1MHz to 120MHz). Those statistical indicators that are mentioned in section 2.3 are calculated for both CM and DM responses.

The Correlation Coefficient measures the similarity between two frequency responses, which are almost 1 in for different (LF, MF, and HF) frequency bands for CM operation of the motor but in DM operation, the value of CC for Cp value of 4.70nF and 6.31nF is quite low showing higher deviation in faulty response. This depicts that there is no significant variation between the responses in CM, but in DM mode, the MF frequency range is greatly affected. The Absolute Sum of Logarithmic Error quantifies deviations in healthy and faulty frequency responses in the logarithmic scale. The higher value of ASLE shows greater deviation with the same amount of impact of the fault in that response. In the calculated values, ASLE is showing an increasing trend with an increase in capacitance value in both CM and DM modes of motor connection, which shows that the increased value of parallel capacitance shows an increased effect of the fault. In CM mode, the HF band is less affected, and in DM mode, the LF band is less affected by faults. The Standard Deviation calculates the spread of the deviation over the applied frequency range, and its higher value indicates more variation in the response, which shows a higher impact of the fault. The SD shows an increasing trend with the increase in value of Cp in both the motor's CM and DM electrical configurations, and its value is lowest in the HF range in CM operation, while the value of SD is smaller in the HF range also in DM operation. The highest value of SD in the MF range for DM shows that this range is most affected by the fault in DM operation, which signifies the MF range is most suitable to measure the severity due to a stator inter-turn fault of an IM. The Mean Squared Error signifies squared differences between the fingerprint response and faulty response, whose higher value shows the response is greatly altered by the inter-turn fault. In CM connection, the MSE is higher in the LF and MF frequency bands compared to the HF frequency range, meaning the low-to-medium frequency range is greatly affected by inter-turn fault, but in DM mode, the

low-frequency band has comparatively lower values of MSE, showing the LF band is less affected by the inter-turn fault while the motor is running in DM mode.

From the values of statistical indicators shown in Tables 4.1 and 4.2, as the capacitance value Cp increases, the values of ASLE, SD, and MSE increase, making fault detection easier. The mid-frequency range is the most sensitive to detecting the effect of a turn fault in the stator of an induction motor, as it has the highest values of SD and MSE.

4.4.1 Statistical Indicators for Common Mode Connection of the Motor

Table 4.1 *Statistical Indicators for Analyzing Faults in Motor while the Motor is in CM*

For Capacitance of 1.75nF			
Frequency range Stats	LF (20Hz-1KHz)	MF (1KHz-1MHz)	HF 1MHz-120MHz
CC	1.00	1.00	0.999
ASLE	0.0064	0.0046	0.0017
SD	1.737	2.86	0.1637
MSE	6.225	12.156	1.2017
For Capacitance of 2.15nF			
Frequency range Stats	LF (20Hz-1KHz)	MF (1KHz-1MHz)	HF 1MHz-120MHz
CC	1.00	1.00	0.999
ASLE	0.0071	0.0059	0.0025
SD	1.906	3.26	0.273
MSE	7.285	16.28	3.088
For Capacitance of 3.3nF			
Frequency range Stats	LF (20Hz-1KHz)	MF (1KHz-1MHz)	HF 1MHz-120MHz
CC	1.00	1.00	0.999
ASLE	0.009	0.0071	0.002
SD	2.461	4.238	0.256
MSE	11.938	26.586	2.1623
For Capacitance of 4.70nF			
Frequency range Stats	LF (20Hz-1KHz)	MF (1KHz-1MHz)	HF 1MHz-120MHz
CC	1.00	1.00	0.9997
ASLE	0.0106	0.0081	0.0037
SD	2.911	4.927	0.411
MSE	16.598	35.596	2.676

4.4.2 Statistical Indicators for Differential Mode Connection of the Motor

Table 4.2 *Statistical Indicators for Analyzing Faults in a Motor while the Motor is in DM*

For Capacitance of 1.80nF			
Frequency range Stats	LF (20Hz-1KHz)	MF (1KHz-1MHz)	HF 1MHz-120MHz
CC	1.00	0.9496	0.9644
ASLE	0.0164	0.0698	0.174
SD	3.312	5.259	3.349
MSE	8.114	30.035	5.256
For Capacitance of 2.10nF			
Frequency range Stats	LF (20Hz-1KHz)	MF (1KHz-1MHz)	HF 1MHz-120MHz
CC	1.00	0.8607	0.9527
ASLE	0.0165	0.1151	0.1928
SD	6.531	13.042	2.735
MSE	7.971	18.875	37.091
For Capacitance of 4.70nF			
Frequency range Stats	LF (20Hz-1KHz)	MF (1KHz-1MHz)	HF 1MHz-120MHz
CC	1.00	0.791	0.9483
ASLE	0.0165	0.1631	0.211
SD	6.469	20.096	3.918
MSE	7.8579	29.727	14.953
For Capacitance of 6.31nF			
Frequency range Stats	LF (20Hz-1KHz)	MF (1KHz-1MHz)	HF 1MHz-120MHz
CC	1.00	0.6145	0.9468
ASLE	0.0162	0.2182	0.217
SD	6.242	27.671	4.318
MSE	7.399	38.127	15.256

Chapter 5 Conclusion and Recommendations

Induction machines are susceptible to various faults throughout their operational lifespan, primarily due to fluctuating operating conditions. A stator short circuits rank among the most serious faults encountered in electrical machines, capable of causing severe damage to the machine and leading to significant financial losses. An inter-turn fault often marks the onset of a stator winding short-circuit, and if not promptly identified, it may evolve into more critical faults such as phase-to-phase or phase-to-ground failures. Traditional fault detection methods are often inadequate for identifying these early-stage faults due to their low sensitivity. In contrast, the Frequency Response Analysis (FRA) method is an efficient tool for diagnosing these faults, providing valuable insights into the condition of the stator winding, offering high dynamic range, accuracy, sensitivity, and safety.

The stator of an electric motor can be represented as an intricate network of resistors (R), inductors (L), and capacitors (C), each with a distinct frequency response under typical operating conditions. Any change in the electrical or mechanical state of the motor can cause deviations in this frequency response. An impedance analyzer can be used to measure this response. The machine’s response under normal operating conditions serves as its "fingerprint." By comparing the frequency response across a supplied frequency range with this fingerprint, it is possible to determine whether the motor is in proper working order or exhibiting malfunctions.

In this study, a frequency sweep ranging from 20 Hz to 120 MHz was applied to analyze the impedance response of the motor in both optimal and malfunctioning states. A fault was induced by progressively increasing the value of a variable capacitor connected in parallel with one of the phases. The results revealed that when a turn-to-turn fault arises within the stator's winding structure due to insulation degradation, resonance is observed at a lower frequency, accompanied by a reduction in impedance magnitude. This phase transition becomes more unstable, signifying a loss of insulation integrity. The increase in the capacitance of the insulating material serves as a strong indicator of insulation degradation.

The obtained statistical indicators showed that as the capacitance value increases, the values of ASLE, SD, and MSE increase, which proves that an increase in the capacitance is the major cause of such a short-circuit. The MF range is the most

affected and is the most sensitive range for identifying turn-to-turn faults in the stator since this range in both CM and DM connections has the most SD and MSE values.

This technique of fault diagnosis is a mature technique that is frequently used in power transformer fault detection and is still under study in the case of rotating machines. Currently, FRA is used as an offline technique for fault diagnosis, but with advanced data acquisition systems, it could be used as an online condition monitoring technique. Future advancements in real-time impedance measurement by incorporating machine learning and the impedance analysis using the FRA technique could be an industry-standard method of fault diagnosis and preventive maintenance.

References

[1] “MACHINERY CONDITION MONITORING PRINCIPLES AND PRACTICES.”

[2] “IET POWER AND ENERGY SERIES 56 Condition Monitoring of Rotating Electrical Machines.”

[3] A. Siddique, G. S. Yadava, and B. Singh, “A review of stator fault monitoring techniques of induction motors,” 2005. doi: 10.1109/TEC.2004.837304.

[4] S. Halder, S. Bhat, D. Zychma, and P. Sowa, “Broken Rotor Bar Fault Diagnosis Techniques Based on Motor Current Signature Analysis for Induction Motor—A Review,” Nov. 01, 2022, *MDPI*. doi: 10.3390/en15228569.

[5] M. Lachance-Savard and É. De, “DIELECTRIC FREQUENCY RESPONSE ANALYSIS APPLIED TO STATOR WINDING INSULATION SYSTEMS,” 2024.

[6] J. Boniface, “Application of Sweep Frequency Response Analysis and Locked-Rotor Test for Stator Winding Inter-Turn and Broken Rotor Bar Fault Detection of Squirrel-Cage Induction Motors,” 2021.

[7] B. Mirafzal, G. L. Skibinski, R. M. Tallam, D. W. Schlegel, and R. A. Lukaszewski, “Universal induction motor model with low-to-high frequency-response characteristics,” *IEEE Trans Ind Appl*, vol. 43, no. 5, pp. 1233–1246, Sep. 2007, doi: 10.1109/TIA.2007.904401.

[8] R. Sadeghi, H. Samet, and T. Ghanbari, “Detection of Stator Short-Circuit Faults in Induction Motors Using the Concept of Instantaneous Frequency,” *IEEE Trans Industr Inform*, vol. 15, no. 8, 2019, doi: 10.1109/TII.2018.2881921.

[9] S. M. Al-Ameri *et al.*, “Application of Frequency Response Analysis Method to Detect Short-Circuit Faults in Three-Phase Induction Motors,” *Applied Sciences (Switzerland)*, vol. 12, no. 4, 2022, doi: 10.3390/app12042046.

[10] G. M. J. Joksimovic´, and J. Penman, “The Detection of Inter-Turn Short Circuits in the Stator Windings of Operating Motors,” 2000.

[11] S. H. Im and B. G. Gu, “Study of Induction Motor Inter-Turn Fault Part I: Development of Fault Models with Distorted Flux Representation,” *Energies (Basel)*, vol. 15, no. 3, Feb. 2022, doi: 10.3390/en15030894.

[12] A. Sharma, S. Chatterji, and L. Mathew, “A Novel Park’s Vector Approach for Investigation of Incipient Stator Fault Using MCSA in Three-Phase Induction Motors.”

[13] M. Otero, P. M. De La Barrera, G. R. Bossio, and R. Leidhold, “Stator inter-turn faults diagnosis in induction motors using zero-sequence signal injection,” *IET Electr Power Appl*, vol. 14, no. 14, pp. 2731–2738, Dec. 2020, doi: 10.1049/iet-epa.2020.0461.

[14] H. Cherif, A. Benakcha, A. Khechekhouche, A. Menacer, S. E. Chehaidia, and H. Panchal, “Experimental diagnosis of inter-turns stator fault and unbalanced voltage supply in induction motor using MCSA and DWER,” vol. 8, no. 3, pp. 1202–1216, 2020.

[15] T. G. Vilhekar, M. S. Ballal, and B. S. Umre, “Application of Sweep Frequency Response Analysis for the detection of winding faults in induction motor,” in *IECON Proceedings (Industrial Electronics Conference)*, 2016. doi: 10.1109/IECON.2016.7793565.

[16] S. M. Al-Ameri *et al.*, “Frequency Response Analysis: An Enabling Technology to Detect Internal Faults within Critical Electric Assets,” *Applied Sciences (Switzerland)*, vol. 12, no. 18, 2022, doi: 10.3390/app12189201.

[17] M. Beheshti Asl, I. Fofana, F. Meghnefi, Y. Brahami, and J. P. D. C. Souza, “A Comprehensive Review of Transformer Winding Diagnostics: Integrating Frequency Response Analysis with Machine Learning Approaches,” *Energies (Basel)*, vol. 18, no. 5, p. 1209, Mar. 2025, doi: 10.3390/en18051209.

[18] S. Plotz, L. Ranzinger, and S. Uhrig, “Frequency Response Analysis on Rotating Machines - Model Parameterization for Different Machine Types and Performance Classes,” in *Diagnostika 2024 - 2024 International Conference on Diagnostics in Electrical Engineering, Proceedings*, Institute of Electrical and Electronics Engineers Inc., 2024. doi: 10.1109/Diagnostika61830.2024.10693894.

[19] L. Ranzinger, S. Uhrig, and S. Tenbohlen, “Analysis and Modeling the Frequency Response of Rotating Machines Regarding Fault Diagnosis Using SFRA,” *IEEE Transactions on Energy Conversion*, vol. 39, no. 1, 2024, doi: 10.1109/TEC.2023.3315341.

[20] F. Perisse, P. Werynski, and D. Roger, “F. Perisse et al.: A New Method for AC Machine Turn Insulation Diagnostic Based on High Frequency Resonances A New Method for AC Machine Turn Insulation Diagnostic Based on High Frequency Resonances,” 2007.

[21] M. Brandt, M. Gutten, and S. Kaščák, “Diagnostic of induction motor using SFRA method,” in *Proceedings of the International Conference - 2016 Conference on Diagnostics in Electrical Engineering, Diagnostika 2016*, 2016. doi: 10.1109/DIAGNOSTIKA.2016.7736474.

[22] F. R. Blanquez, C. A. Platero, E. Rebollo, and F. Blanquez, “Evaluation of the applicability of FRA for inter-turn fault detection in stator windings,” in *Proceedings - 2013 9th IEEE International Symposium on Diagnostics for Electric Machines, Power Electronics and Drives, SDEMPED 2013*, 2013. doi: 10.1109/DEMPED.2013.6645714.

[23] Zbigniew. Leonowicz, *Conference proceedings : 2020 IEEE International Conference Environment and Electrical Engineering and 2020 IEEE Industrial and Commercial Power Systems Europe (EEEIC*. IEEE, 2020.

[24] G. Vidmar and D. Miljavec, “A Universal High-Frequency Three-Phase Electric-Motor Model Suitable for the Delta- and Star-Winding Connections,” *IEEE Trans Power Electron*, vol. 30, no. 8, 2015, doi: 10.1109/TPEL.2014.2352452.

[25] M. S. Toulabi, L. Wang, L. Bieber, S. Filizadeh, and J. Jatskevich, “A universal high-frequency induction machine model and characterization method for arbitrary stator winding connections,” *IEEE Transactions on Energy Conversion*, vol. 34, no. 3, 2019, doi: 10.1109/TEC.2019.2891349.

[26] I. Stevanovic, B. Wunsch, and S. Skibin, “Behavioral high-frequency modeling of electrical motors,” in *Conference Proceedings - IEEE Applied Power Electronics Conference and Exposition - APEC*, 2013. doi: 10.1109/APEC.2013.6520654.

[27] J. Sun and L. Xing, “Parameterization of three-phase electric machine models for EMI simulation,” *IEEE Trans Power Electron*, vol. 29, no. 1, pp. 36–41, 2014, doi: 10.1109/TPEL.2013.2264750.

[28] N. Idir, Y. Weens, M. Moreau, and J. J. Franchaud, “High-frequency behavior models of AC motors,” *IEEE Trans Magn*, vol. 45, no. 1, 2009, doi: 10.1109/TMAG.2008.2006006.

[29] G. Grandi, S. Profile, and A. Massarini, “High frequency lumped parameter model for AC motor windings,” 1997. [Online]. Available: https://www.researchgate.net/publication/233728785

[30] . IEEE Staff, *2012 XXth International Conference on Electrical Machines*. IEEE, 2012.

[31] O. Magdun and A. Binder, “High-frequency induction machine modeling for common mode current and bearing voltage calculation,” in *IEEE Transactions on Industry Applications*, Institute of Electrical and Electronics Engineers Inc., 2014, pp. 1780–1790. doi: 10.1109/TIA.2013.2284301.

[32] . IEEE Staff, *2012 XXth International Conference on Electrical Machines*. IEEE, 2012.

[33] S. M. A. N. Al-Ameri *et al.*, “Understanding the Influence of Power Transformer Faults on the Frequency Response Signature Using

Simulation Analysis and Statistical Indicators," *IEEE Access*, vol. 9, pp. 70935–70947, 2021, doi: 10.1109/ACCESS.2021.3076984.

[34] M. H. Samimi, S. Tenbohlen, A. A. S. Akmal, and H. Mohseni, "Evaluation of numerical indices for the assessment of transformer frequency response," *IET Generation, Transmission and Distribution*, vol. 11, no. 1, pp. 218–227, Jan. 2017, doi: 10.1049/iet-gtd.2016.0879.

[35] M. Tahir, S. Tenbohlen, and M. H. Samimi, "Evaluation of Numerical Indices for Objective Interpretation of Frequency Response to Detect Mechanical Faults in Power Transformers," in *Lecture Notes in Electrical Engineering*, Springer Science and Business Media Deutschland GmbH, 2020, pp. 811–824. doi: 10.1007/978-3-030-31676-1_76.

Appendix-A

Optimal Values of the Parameters Used for High-Frequency Modeling of the Machine

Parameters	Unit	Value
C_{G1}	pF	221
C_{G2}	pF	597
R_{G1}	Ω	4.5
R_{G2}	kΩ	4.17
R_S	Ω	19.69
L_S	mH	80.05
R_E	kΩ	17.71
C_T	pF	30.9
L_T	mH	97.19
R_T	kΩ	13.975
L_C	nH	45.7

Appendix B

MATLAB model and its connection to CM and DM operation

1. Common Mode Connection

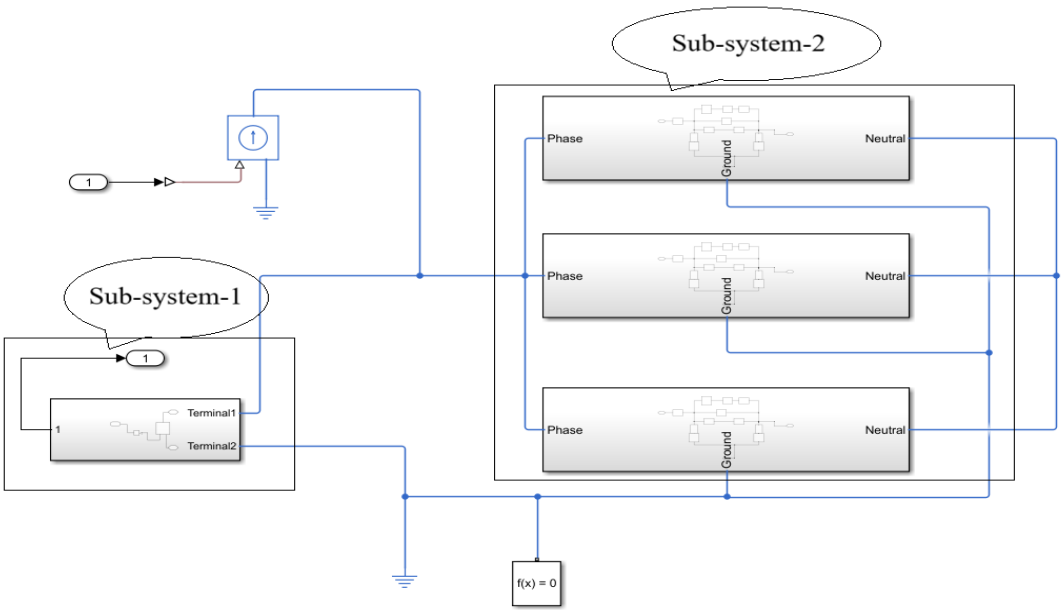

Figure: CM Connection of Model in MATLAB

2. Differential Mode Connection

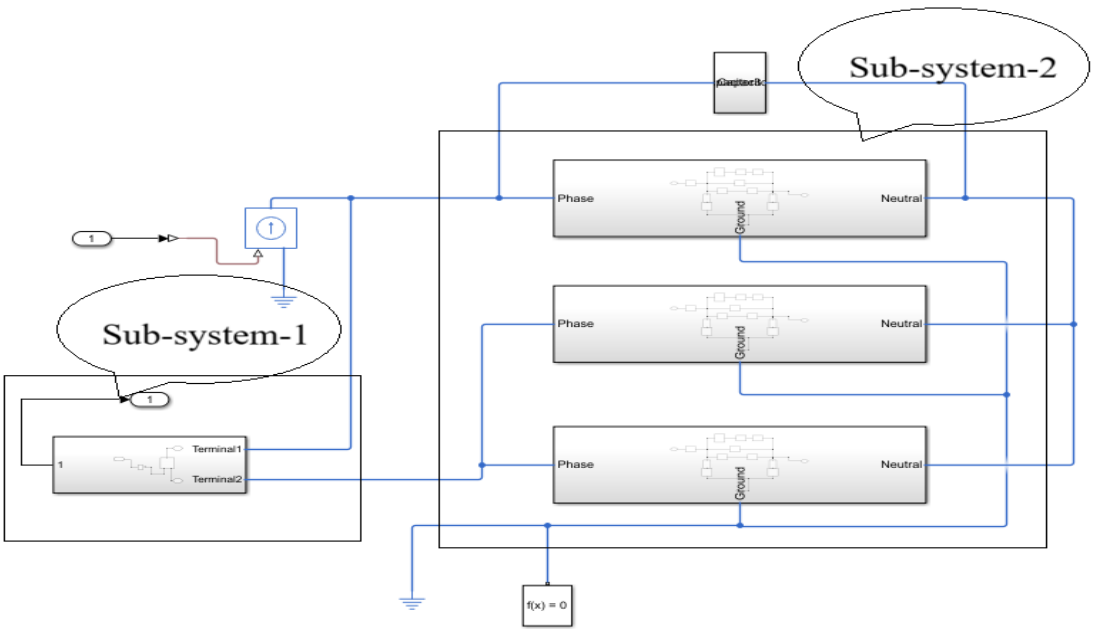

Figure: DM Connection of Model in MATLAB

3. The expanded view of sub-system-2 shown in both connection modes is shown below:

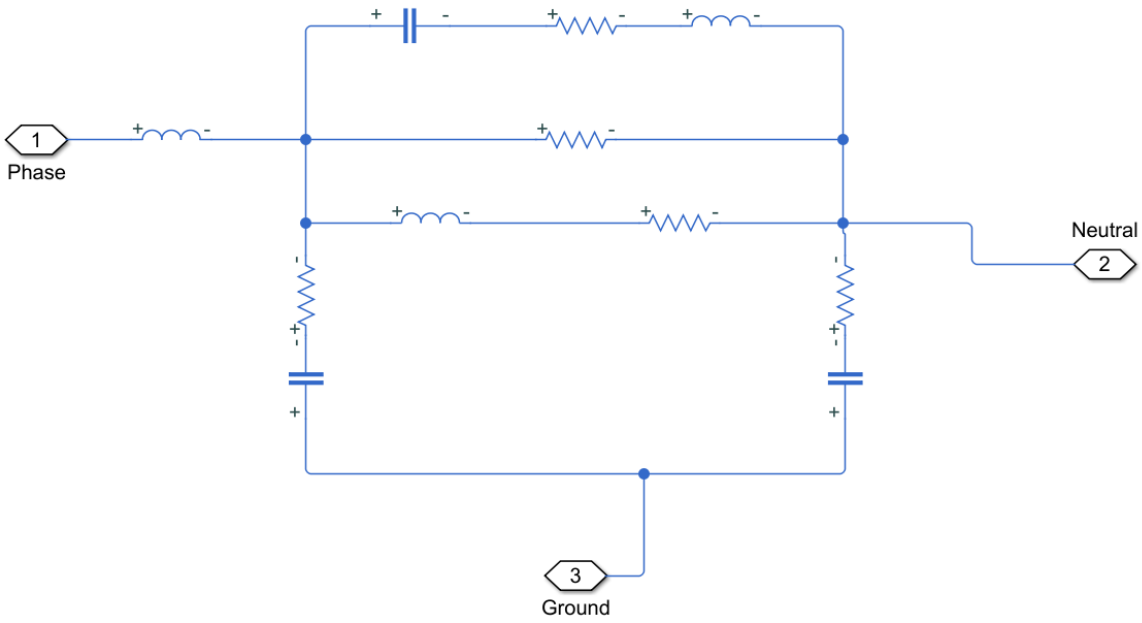

Figure: High-Frequency Model with Terminal Points that is Used in Sub-system-2

Appendix C

1. MATLAB Codes used for Signal Analysis of Experimental Data

   (i) For healthy case signal analysis

```
%% Loading Practical Data
data1 = readtable('lab_motor_response.xlsx');
frequency_dmtest = data1.frequency_1;  % Healthy case frequency data
Zdm_test = data1.Zdm_test;  % Healthy impedance data (Ohms)
data2 = readtable('HEALTHY_CM.CSV');
frequency_cmtest = data2.Frequency;  % CM case frequency data
Zcm_test = data2.Z_cm;  % CM impedance data (Ohms)
%% Creation of Figure for Magnitude and Phase Response
% Magnitude Plot
figure('Name', 'Frequency Response of Differential Mode vs Common Mode');
hold on;
plot(frequency_dmtest, abs(Zdm_test), 'k', 'LineWidth', 1);  % DM magnitude
plot(frequency_cmtest, abs(Zcm_test), 'g', 'LineWidth', 1);  % CM magnitude
grid on;
ylabel('Impedance (Ohms)');
xlabel('Frequency (Hz)');
title('Magnitude Response (Differential vs Common Mode)');
legend('Differential Mode Response', 'Common Mode Response');
set(gca, 'XScale', 'log', 'YScale', 'log');
xlim([20, 120e6]);
hold off;
% Phase Plot
hold on;
plot(frequency_dmtest, Phase_dm_test, 'k', 'LineWidth', 1);  % Healthy case phase
plot(frequency_cmtest, Phase_cm_test, 'g', 'LineWidth', 1);  % Degraded case phase
grid on;
ylabel('Phase (Degrees)');
xlabel('Frequency (Hz)');
```

```
title('Phase Response (Differential vs Common Mode)');
legend('Differential Mode Response', 'Common Mode Response');
set(gca, 'XScale', 'log');
xlim([20, 12e6]);
hold off;
```

(ii) Signal analysis for different conditions

```
%% Loading Practical Data
data = readtable('lab_motor_response.xlsx');
frequency_practical = data.frequency1;  % Healthy frequency data
Zdm_test = data.Zdm_test;  % Healthy impedance data (Ohms)
data1 = readtable('0-750NF.CSV');
frequency_degraded1 = data1.Frequency;
Z_degraded1 = data1.Z;
data2 = readtable('1-80NFB.CSV');
frequency_degraded2 = data2.Frequency;
Z_degraded2 = data2.Z;
data3 = readtable('2-14NFB.CSV');
frequency_degraded3 = data3.Frequency;
Z_degraded3 = data3.Z;
data4 = readtable('4-700NF.CSV');
frequency_degraded4 = data4.Frequency;
Z_degraded4 = data4.Z;
data5 = readtable('6-310NF.CSV');
frequency_degraded5 = data5.Frequency;
Z_degraded5 = data5.Z;
data6 = readtable('8-200NF.CSV');
frequency_degraded6 = data6.Frequency;
Z_degraded6 = data6.Z;
%% Creation Figure for Magnitude and Phase Response
figure('Name', 'Frequency Response of Healthy vs Degraded Cases');
```

```
%% Magnitude Plot
hold on;
plot(frequency_practical, abs(Zdm_test), 'k', 'LineWidth', 1.5); % Healthy case magnitude
plot(frequency_degraded1, abs(Z_degraded1), 'g', 'LineWidth', 1.5); % Degraded case1
plot(frequency_degraded2, abs(Z_degraded2), 'r', 'LineWidth', 1.5); % Degraded case2
plot(frequency_degraded3, abs(Z_degraded3), 'b', 'LineWidth', 1.5); % Degraded case3
plot(frequency_degraded4, abs(Z_degraded4), 'y', 'LineWidth', 1.5); % Degraded case4
plot(frequency_degraded5, abs(Z_degraded5), 'm', 'LineWidth', 1.5); % Degraded case5
plot(frequency_degraded6, abs(Z_degraded6), 'c', 'LineWidth', 1.5); % Degraded case6
grid on;
ylabel('Impedance (Ohms)');
xlabel('Frequency (Hz)');
title('Magnitude Response (Healthy vs Degraded)');
legend('Healthy Response', 'Response with Prallel Cp 0.7nF ', 'Response with Parallel Cp 1.8nF', 'Response with Prallel Cp 2.14nF', 'Response with Prallel Cp 4.7nF', 'Response with Prallel Cp 6.31nF', 'Response with Prallel Cp 8.2nF');
set(gca, 'XScale', 'log', 'YScale', 'log');
xlim([20, 120e6]);
hold off;
%% Phase Plot
hold on;
plot(frequency_practical, Phase_dm_test, 'k', 'LineWidth', 1); % Healthy case phase
plot(frequency_degraded1, Phase_degraded1, 'g', 'LineWidth', 1); % Degraded case1
plot(frequency_degraded2, Phase_degraded2, 'r', 'LineWidth', 1); % Degraded case2
plot(frequency_degraded3, Phase_degraded3, 'b', 'LineWidth', 1); % Degraded case3
plot(frequency_degraded4, Phase_degraded4, 'y', 'LineWidth', 1); % Degraded case4
plot(frequency_degraded5, Phase_degraded5, 'm', 'LineWidth', 1); % Degraded case5
plot(frequency_degraded6, Phase_degraded6, 'c', 'LineWidth', 1); % Degraded case6
```

```
grid on;
ylabel('Phase (Degrees)');
xlabel('Frequency (Hz)');
title('Phase Response (Healthy vs Degraded)');
legend('Healthy Response', 'Response with Prallel Cp 0.7nF ', 'Response with Parallel Cp 1.8nF', 'Response with Prallel Cp 2.14nF', 'Response with Prallel Cp 4.7nF', 'Response with Prallel Cp 6.31nF', 'Response with Prallel Cp 8.2nF');
set(gca, 'XScale', 'log');
xlim([20, 16e6]);
hold off;
```

2. MATLAB Codes used for model simulation

(i) Common and Differential mode simulation of model

```
%  Define the optimal parameters for the model
Req = 19.69;
Leq = 80.05e-3;
Cg1 = 221e-12;
Cg2 = 597e-12;
Rg1 = 4.5;
Rg2 = 4.17e3;
Re = 17.71e3;
Ct = 30.9e-12;
Lt = 97.19e-3;
Rt = 13.975e3;
Lc = 45.7e-09;
%% Open the model and set circuit parameters
open_system('IM_model_for_CM_mode')
open_system('IM_model_for_DM_mode')
%% Linearize the model
[a, b, c, d] = linmod('IM_model_for_CM_mode');
clear simlog_IM_model_for_CM_mode
[a1, b1, c1, d1] = linmod('IM_model_for_DM_mode');
clear simlog_IM_model_for_DM_mode
```

```
%% Bode plot of the linearized model (in Ohms)
npts = 500;
f = logspace(1, 10, npts);  % Frequency range from 1 Hz to 10^8 Hz
G = zeros(1, npts);
G1 = zeros(1, npts);
for i = 1:npts
G(i) = c*(2*pi*1i*f(i)*eye(size(a))-a)^-1*b +d;
G1(i) = c1*(2*pi*1i*f(i)*eye(size(a1))-a1)^-1*b1 +d1;
end
%% Create Figure for Magnitude and Phase Response
figure('Name', 'Frequency Response of IM Model');
%% Magnitude Plot (Subplot 1)
subplot(2,1,1);
hold on;
plot(f, abs(G), 'r-', 'LineWidth', 1);  % Model impedance magnitude
plot(f, abs(G1), 'k', 'LineWidth', 1);  % Practical impedance magnitude
grid on;
ylabel('Impedance (Ohms)');
xlabel('Frequency (Hz)');
title('Magnitude Response');
legend('common mode', 'differential mode');
set(gca, 'XScale', 'log', 'YScale', 'log');
xlim([20, 120e6]);
hold off;
%% Phase Plot (Subplot 2)
subplot(2,1,2);
hold on;
plot(f, angle(G) * (180/pi), 'r-', 'LineWidth', 1);  % Model phase in degrees
plot(f, angle(G1) * (180/pi), 'k', 'LineWidth', 1);  % Practical phase data
grid on;
ylabel('Phase (Degrees)');
xlabel('Frequency (Hz)');
title('Phase Response');
legend('common mode', 'differential mode');
```

```
set(gca, 'XScale', 'log');
xlim([20, 120e6]);
hold off;
```

(ii) Model Verification with Data

```
% Define the optimal parameters for the motor model
Req = 19.69;
Leq = 80.05e-3;
Cg1 = 221e-12;
Cg2 = 597e-12;
Rg1 = 4.5;
Rg2 = 4.17e3;
Re = 17.71e3;
Ct = 30.9e-12;
Lt = 97.19e-3;
Rt = 13.975e3;
Lc = 45.7e-09;
%% Open the model and set circuit parameters
open_system('IM_model_for_DM_mode')
%% Linearize the model
[a, b, c, d] = linmod('IM_model_for_DM_mode');
clear simlog_IM_model_for_DM_mode
%% Bode plot of the linearized model (in Ohms)
npts = 500;
f = logspace(0, log10(120e6), npts);  % Frequency range from 1 Hz to 10^8 Hz
G = zeros(1, npts);
for i = 1:npts
G(i) = c * ((2 * pi * 1i * f(i) * eye(size(a))) - a)^-1 * b + d;
end
%% Load Practical Data (from 'lab_motor_response.xlsx')
data = readtable('lab_motor_response.xlsx');
frequency_practical = data.frequency_1;  % Practical frequency data
Zdm_test = data.Zdm_test;  % Practical impedance data (in Ohms)
Phase_dm_test = data.Phase_dm_test;  % Practical phase response (in degrees)
```

```
%% Create Figure for Magnitude and Phase Response
figure('Name', 'Frequency Response of IM Model');
%% Magnitude Plot (Subplot 1)
subplot(2,1,1);
hold on;
plot(f, abs(G), 'r-', 'LineWidth', 1);  % Model impedance magnitude
plot(frequency_practical, abs(Zdm_test), 'k', 'LineWidth', 1);  % Practical impedance magnitude
grid on;
ylabel('Impedance (Ohms)');
xlabel('Frequency (Hz)');
title('Magnitude Response');
legend('common mode', 'differential mode');
set(gca, 'XScale', 'log', 'YScale', 'log');
xlim([20, 120e6]);
hold off;
%% Phase Plot (Subplot 1)
subplot(2,1,2);
hold on;
plot(f, angle(G) * (180/pi), 'r-', 'LineWidth', 1);  % Model phase in degrees
plot(frequency_practical, Phase_dm_test, 'k', 'LineWidth', 1);  % Practical phase data
grid on;
ylabel('Phase (Degrees)');
xlabel('Frequency (Hz)');
title('Phase Response');
legend('Model Response', 'Practical Data');
set(gca, 'XScale', 'log');
xlim([20, 120e6]);
hold off;
```

(iii) Model simulation for variable capacitors

```
%% Define Initial Parameters for Motor Model
Req = 19.69;
```

```
Leq = 80.05e-3;
Cg1 = 221e-12;
Cg2 = 597e-12;
Rg1 = 4.5;
Rg2 = 4.17e3;
Re = 17.71e3;
Ct = 30.96e-12;
Lt = 97.19e-3;
Rt = 13.975e3;
Lc = 45.7e-09;
%% Define Variable Cp Values
Cp_values = [0.001e-12, 0.75e-9, 1.80e-9, 2.14e-9, 4.70e-9, 6.31e-9, 8.20e-9];
colors = ['b', 'y', 'c', 'r', 'g', 'm', 'k'];  % Fixed missing comma issue
%% Open the Simulink Model
open_system('IM_model_for_DM_mode');
%% Create Figure for Magnitude and Phase Response
figure('Name', 'Frequency Response of IM Model with Variable Cp');
%% Initialize Frequency Range for Analysis
npts = 500;
f = logspace(1, 10, npts);  % Frequency range from 10 Hz to 10 GHz
%% Loop Over Different Cp Values
for i = 1:length(Cp_values)
Cp = Cp_values(i);  % Set Cp value
% Run Simulation
simOut = sim('IM_model_for_DM_mode', 'StopTime', '1e-3');
% Linearize the model
```

```
[a, b, c, d] = linmod('IM_model_for_DM_mode');
% Compute Frequency Response
G = zeros(1, npts);
for j = 1:npts
G(j) = c * ((2 * pi * 1i * f(j) * eye(size(a))) - a) ^ -1 * b + d;
end
%% Plot Magnitude Response
subplot(2,1,1);
hold on;
plot(f, abs(G), 'Color', colors(i), 'LineWidth', 1);
%% Plot Phase Response
subplot(2,1,2);
hold on;
plot(f, angle(G) * (180/pi), 'Color', colors(i), 'LineWidth', 1);
end
%% Final Formatting for Magnitude Plot
subplot(2,1,1);
grid on;
ylabel('Impedance (Ohms)');
xlabel('Frequency (Hz)');
title('Magnitude Response for Different Cp Values');
legend(arrayfun(@(x) sprintf('Cp = %.2fnF', x*1e9), Cp_values, 'UniformOutput',
false));
set(gca, 'XScale', 'log', 'YScale', 'log');
xlim([20, 120e6]);
%% Final Formatting for Phase Plot
```

```
subplot(2,1,2);
grid on;
ylabel('Phase (Degrees)');
xlabel('Frequency (Hz)');
title('Phase Response for Different Cp Values');
legend(arrayfun(@(x) sprintf('Cp = %.2fnF', x*1e9), Cp_values, 'UniformOutput', false));
set(gca, 'XScale', 'log');
xlim([20, 120e6]);
hold off;
```

3. Statistical Analysis

```
% FRA Data from Excel File
filename = 'cm_fra_for_stats.csv'; % file name
data = readmatrix(filename); % Read the Excel file
frequencies = data(:, 1); % Extract Frequency column
healthy_fra = data(:, 2); % Extract Healthy IM response
faulty_fra = data(:, 3); % Extract Faulty IM response
% Extract Significant Frequency Range (1 kHz – 100 kHz)
freq_range = (frequencies >= 10 & frequencies <= 10e2); % Logical index
filtered_frequencies = frequencies(freq_range);
healthy_filtered = healthy_fra(freq_range);
faulty_filtered = faulty_fra(freq_range);
% Compute Statistical Indicators for Extracted Data
% Correlation Coefficient (CC)
CC = corrcoef(healthy_filtered, faulty_filtered);
CC = CC(1,2); % Extract correlation value
% Average Sum of Logarithmic Errors (ASLE)
ASLE = mean(abs(log10(healthy_filtered) - log10(faulty_filtered)));
```

```
% Standard Deviation (SD)
SD = std(healthy_filtered)-std(faulty_filtered);
% Mean Squared Error (MSE)
MSE = sum((healthy_filtered - faulty_filtered).^2)/length(healthy_filtered);
% Display Results
fprintf('Statistical Indicators for Extracted Frequency Range (10kHz – 3 MHz):\n');
fprintf('Correlation Coefficient (CC): %.4f\n', CC);
fprintf('Average Sum of Logarithmic Errors (ASLE): %.4f\n', ASLE);
fprintf('Standard Deviation (SD): %.4f\n', SD);
fprintf('Mean Squared Error (MSE): %.4f\n', MSE);
```

Appendix D

Publication:

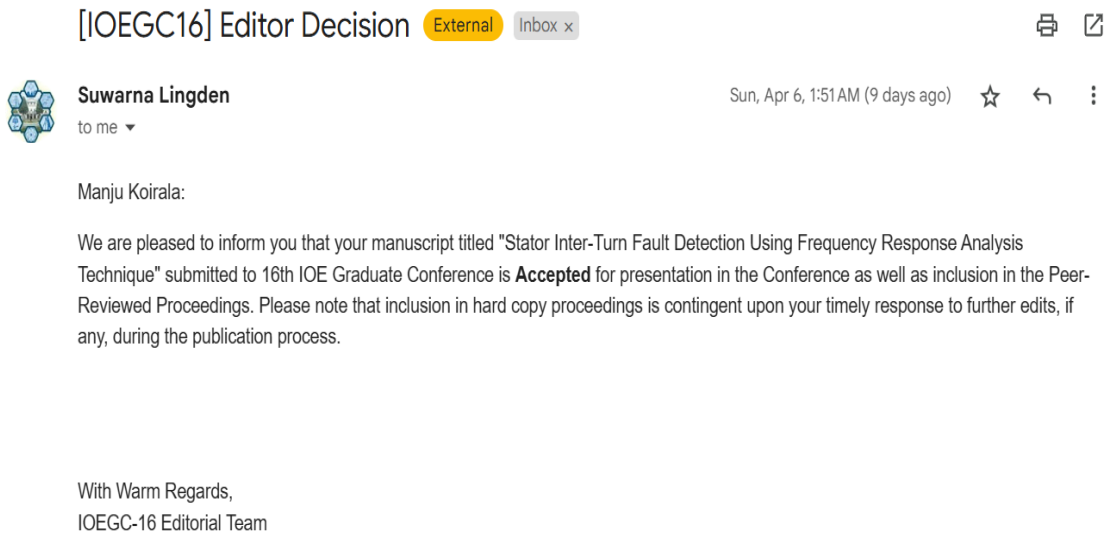

[IOEGC16] Editor Decision External Inbox ×

Suwarna Lingden Sun, Apr 6, 1:51 AM (9 days ago)
to me

Manju Koirala:

We are pleased to inform you that your manuscript titled "Stator Inter-Turn Fault Detection Using Frequency Response Analysis Technique" submitted to 16th IOE Graduate Conference is **Accepted** for presentation in the Conference as well as inclusion in the Peer-Reviewed Proceedings. Please note that inclusion in hard copy proceedings is contingent upon your timely response to further edits, if any, during the publication process.

With Warm Regards,
IOEGC-16 Editorial Team

IOE Graduate Conference
[Placeholder for Publication Information]

Stator Inter-Turn Fault Detection by Analyzing Impedance Using Frequency Response Analysis Technique

Manju Koirala [a], Bishal Silwal [b], Anil Kumar Panjiyar [c], Toomas Vaimann [d], Muhammad Usman Sardar [e]

[a, b, c] *Department of Electrical Engineering, Pulchowk Campus, Tribhuvan University, Nepal*
[d,e] *Department of Power Engineering and Mechatronics, Tallinn University of Technology*
[a] 079mspse012.manju@pcampus.edu.np

Abstract
Stator short-circuit faults accounts near about one-third of the total faults that occurs in Induction Machine. With increased automation of the industrial sector and reduced man-machine interface, the importance of condition monitoring of electrical machines is increasing day by day. The stator short circuit faults often occur due to insulation breakdown as a result of overloading, insulation aging, and mechanical stress, with a local inter-turn fault which creates a supplementary thermal stress and, if not diagnosed, results in phase-to-phase and phase-to-ground faults. For inverter-fed machines, these problems are more frequent and cannot be diagnosed using classical methods. The frequency response analysis technique is suitable for such cases due to its high dynamic range, high accuracy, high sensitivity, and safety.

Keywords
Induction Motor, Condition Monitoring, Frequency Response Analysis

1. Background

Among various rotating electrical machines that are used, the induction motor is the most common. Induction motors are widely used because of their low cost, relatively small size, robustness, low maintenance cost, and high efficiency. It is made mainly of three different components: a) the magnetic core, b) the stator and c) the rotor[1]. Induction machines are the primary drives in the various applications of which squirrel cage induction machine consumes around 85% of power in industrial plant. According to a survey conducted by IEEE and EPRI, it is found that the percentage contribution of stator fault is around 37% among various faults that occur in induction motors[2].

Stator short-circuit faults occur in the form of turn-to-turn, coil-to-coil, phase-to-phase, phase-to-ground that may result in catastrophic machine failures such as unscheduled shutdown and significant expenses of maintenance. An accurate and early detection of stator faults is necessary to prevent catastrophic failures of IMs and relevant side effects[3]. The main cause of such failures is insulation breakdown of the stator winding due to different electrical and mechanical stresses. In case of inter-turn fault, the motor can continue to work but in case of short circuit between two phases motor is not able to work. Thus, if an inter-turn fault cannot be immediately detected, it can be converted to phase-to-phase or a phase-to-earth fault which imposes significant maintenance cost. Condition monitoring is the graphical trend of analyzing machine parameters for the purpose of detection, analysis and correction of machine problems before failure takes place[4].

Ground insulation faults are easily detected by classical method based on leakage current measurement. For large machines, on-line methods based on partial dischagre detection and analysis give good results but they cannot be used for low voltage machines fed by adjustable speed drives. Turn insulation quality evaluation through classical method is difficult, which is the only way to detect very beginning of an insulation problem. When the quality of turn insulation changes because of aging, the resonance frequency changes and variation of capacitance can be considered as an indicator of the turn insulation aging[5]. While emerging short circuit turns within the stator winding will not affect the performance of rotating machine significantly, it can

progress rapidly causing severe damages to the machine. Thus, detecting and correcting such flaws at an early stage is critical[6]

1.1 Stator Winding and Insulation Breakdown

The stator winding is made of several turns of insulated copper conductors which are wrapped around the teeth of the magnetic core. To achieve this, individual coils or bars are inserted inside the stator core where they are connected in series or in parallel to form a complete winding. Stator coils and bars are made of copper which is surrounded with electrical insulation to prevent the conductors which are energized at high voltage potential during operation, from getting in contact with the grounded core. Depending upon the voltage rating, stator windings of different designs are used. For higher rated machines, conductors of high current carrying capacity are needed for which conductors of large cross-section are required which are made from several strands connected in parallel. Each strand must be insulated from each other using a thin insulation layer[1].

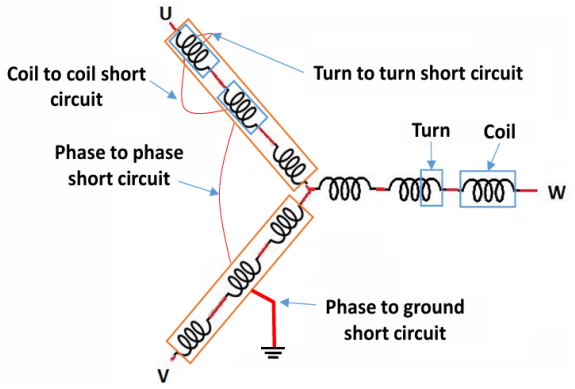

Figure 1: Short circuit faults in Stator of Induction Motor[6]

The occurrence rate of winding insulation fault is high in case of inverter-fed induction motor[1, 5] which is a severe fault type because it is accompanied by high fault current, heat generation, burned windings, burned motors and in the worst case, fire hazards. If the temperature of the stator winding is above the threshold temperature limit, oxidation of insulation occurs, which makes the insulating material brittle and the copper conductor inside the insulator also gets expanded, damaging the coated insulating material. When inverter-fed drives operate machines, inverter with pulse width modulation can invoke surge voltages on the motor winding[1].

1.2 Frequency Response Analysis

Frequency response analysis technique has been recognized worldwide as a matured technology to assess the winding conditions of power transformers[7]. The FRA test is conducted by injecting a low voltage of a wide frequency range at one end of the winding terminals while measuring the response at the other terminal of the winding. FRA advantages include high dynamic range, high accuracy, low energized voltage and high sensitivity and safety[6]. The working principle of FRA technique is to analyze the system's impedance or resonance characteristics over an applied frequency range. There are two fundamental methods to preform FRA in any machine: Sweep Frequency Response Analysis (SFRA) and Impulse Frequency Response Analysis (IFRA). In SFRA, a low voltage sinusoidal signal of varying frequency range (Hz to MHz) is applied in one terminal of a machine and output of the other terminal is measured or analyzed while in IFRA, a high-frequency impulse signal is applied and the response of the system is measured. Compared to IFRA, SFRA may be slower but it is less susceptible to interference, technically easier to implement and provides higher accuracy over wide range of frequency and a non-destructive method of condition monitoring[8].

Stator insulation failure mechanism counts about one-third of the total ac machine failures in industrial application and is often starts with a local turn-to-turn breakdown. For adjustable speed drives (ASD), these problems occur more frequently because turn-to-turn voltage includes spikes that may cause partial discharge which is the origin of an early aging. It is more difficult to evaluate the quality of turn insulation using classical methods, which is only way to detect very beginning of an insulation problem, particularly for inverter-fed machines. When the quality of the turn insulation changes because of aging, the resonance frequency changes and capacitance increases with insulation aging[5].

FRA technique is based on the evaluation of equivalent impedance of the windings in frequency domain. Since a stator winding can be considered as an equivalent circuit with a complex network of capacitance, resistance and inductance, the frequency response is unique and it can be used as a fingerprint of the winding under test. Thus, any physical alteration or electrical modification of the winding results in a variation of the frequency response, which is detected by comparing this test to the reference

frequency response of the winding in healthy condition[9]. Frequency response analysis is mainly a graphical analysis based technique, a visual inspection can be used to detect the variations between indction motor frequency signature and its reference signature[10]

2. Methodology

This section describes the method, tools and technique used to detect the stator turn-to-turn of an induction motor. The input of a signal generator that can produce a signal of 20Hz to 120MHz is applied to the one terminal of IM under test and the response is detected through an impedance analyzer. The experiment was carried out in Department of Electrical Power and Mechatronics at the Tallinn University of Technology, Estonia. The machine (induction motor and impedance analyzer) specifications are shown in Table 1.

Table 1: Specifications of used Machines

Parameters	Unit	Value
Number of Phase		3
Connection		Star
Voltage	V	400
Current	A	1.7
Power	kW	0.75
Speed	rpm	1440
Power Factor		0.76
Frequency range	Hz	$20 - 12 * 10^7$
Impedance range	Ohm	$25 * 10^{-3} - 40 * 10^6$

First, the data for healthy condition were obtained for the mentioned frequency range by connecting the motor in differential and common mode as characterization of IM in high frequency operation requires differential and common mode data. The connection diagram for DM and CM is given in Figure 2.

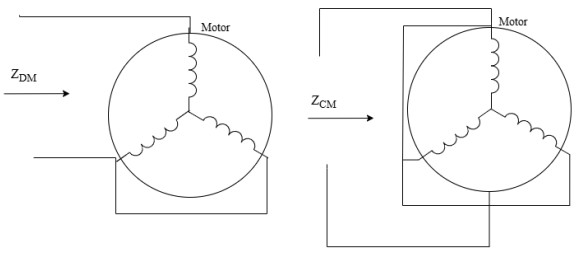

Figure 2: Differential and Common mode connection of motor

A fault was created using with the help of capacitors with variable capacitance which are connected in parallel to a whole winding as various literature states that as the insulation degradation occurs the capacitance of the insulating material increases due to reduction in dielectric property of the material. The signal analysis of the data obtained was performed in MATLAB software.

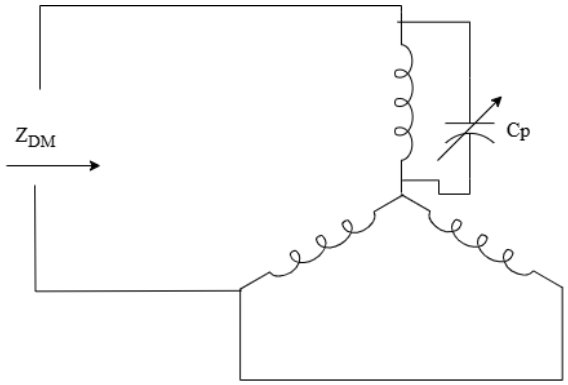

Figure 3: Schematic of fault creation in lab

The block diagram of the complete process is shown in Figure 4

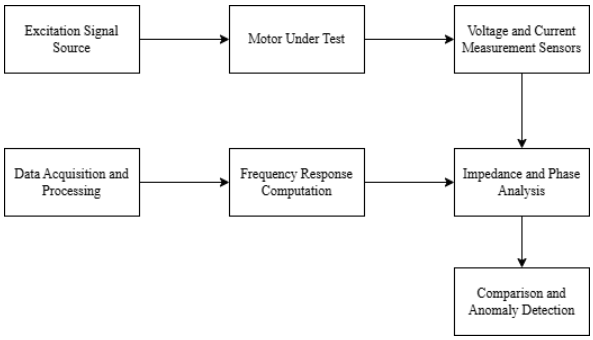

Figure 4: Block diagram of the complete process

3. Results and Discussion

Figure 5 – 10 shows the results of impedance analysis of the star-connected stator winding of induction motor. Figure 5 can be used as the fingerprint as it is the result of normal operating conditions.

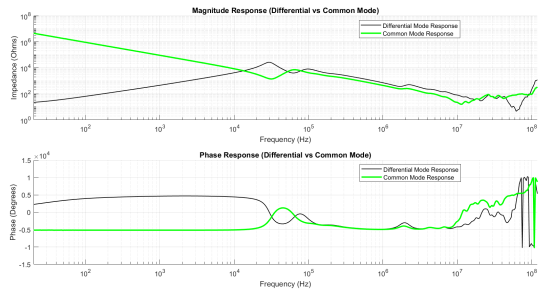

Figure 5: Magnitude and Phase response of differential and common mode connection of motor

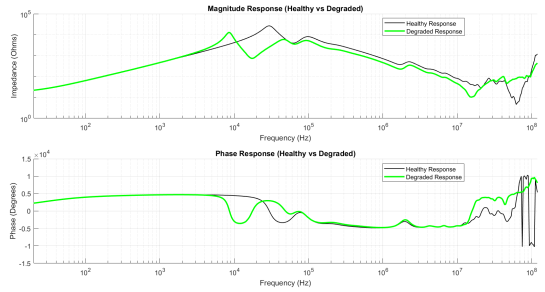

Figure 6: Comparing response of normal operation with faulty one in degraded case

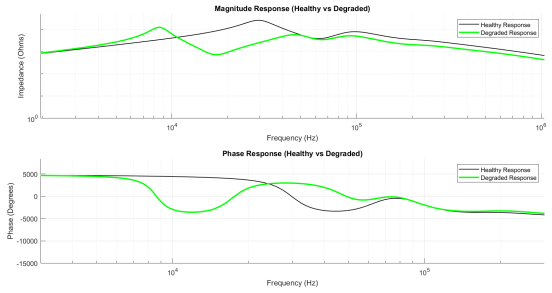

Figure 7: Zoomed graph that shows the resonance phenomena in healthy and faulty case

In Figure 5- 7, it is clearly seen that the response shifts to the left in the event of insulation degradation between turns, indicating a reduction in the effective inductance caused by inter-turn faults. This shift strongly shows that the electrical circuit parameters are changed due to short circuits in the winding. In degraded response, resonance peaks are less pronounced, suggesting increased energy dissipation due to circulating currents that are generated due to inter-turn fault. This might be a case of low impedance path which is a characteristic of inter-turn fault.

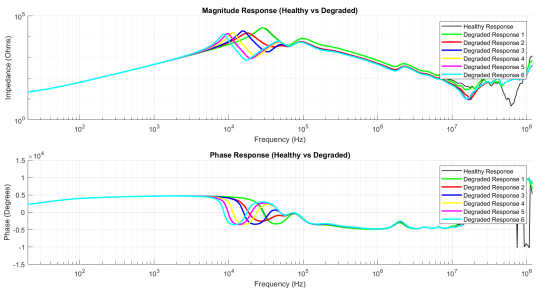

Figure 8: Magnitude and Phase response of normal and degraded cases in different mode

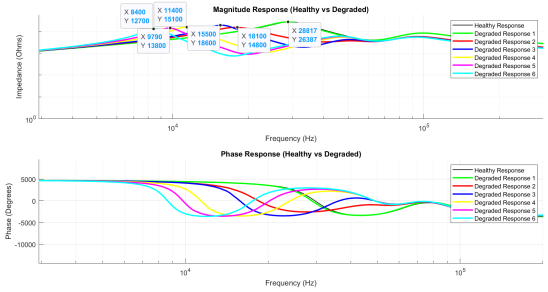

Figure 9: Resonance phenomena for different cases

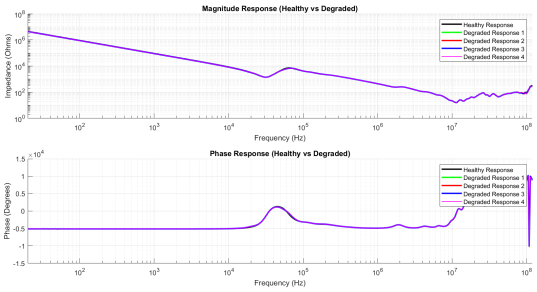

Figure 10: Magnitude and Phase response of different cases of common mode connection of motor

In Figure 8- 9, it is clear that the magnitude response shows a deviation that confirms changes in the electrical parameters of the stator. At higher frequencies, the fluctuation of the response of the degraded cases shows an increase in parasitic capacitance and leakage currents in the faulty winding. The phase response shows a phase lead at lower frequencies indicating altered inductance, which points an imbalance in the mutual coupling of winding conforming the presence of inter-turn fault. The unstable phase response beyond the frequency of 10^7 Hz shows a localized insulation failure that could progress to more severe damage. In Figure 10, it is seen that the common mode connection is not suitable for detecting inter-turn faults caused by insulation

degradation.

This technique of fault diagnosis is a matured technique that is frequently used in power transformer fault detection and is still under study in the case of rotating machine. Currently, FRA is used as an offline technique for fault diagnosis, but with advanced data acquisition systems, it could be used as online condition monitoring technique. Future advancements in real-time impedance measurement by incorporating machine learning, the impedance analysis using FRA technique could be an industry-standard method of fault diagnosis and preventive maintenance.

4. Conclusion

From the above discussion, we can say that if an inter-turn fault occurs in a stator winding due to insulation degradation, resonance occurs at lower frequency with decreased magnitude of impedance. The phase transition becomes more unstable, indicating loss of insulation integrity. The response of the normal operating condition can be used as the fingerprint to compare the responses of various cases as every operating condition has its unique frequency response.

Acknowledgments

This study was supported by Department of Electrical Power Engineering and Mechatronics, Tallinn University of Technology under the project Capacity Enhancement in Electrical Equipment Condition Monitoring and Fault Diagnosis (CEEECoM).

References

[1] Mathieu Lachance-Savard. *Dielectric frequency response analysis applied to stator winding insulation systems*. PhD thesis, Ecole de technologie superieure, 2024.

[2] Sudip Halder, Sunil Bhat, Daria Zychma, and Pawel Sowa. Broken rotor bar fault diagnosis techniques based on motor current signature analysis for induction motor—a review. *Energies*, 15(22):8569, 2022.

[3] Reza Sadeghi, Haidar Samet, and Teymoor Ghanbari. Detection of stator short-circuit faults in induction motors using the concept of instantaneous frequency. *IEEE Transactions on Industrial Informatics*, 15(8):4506–4515, 2018.

[4] Arfat Siddique, GS Yadava, and Bhim Singh. A review of stator fault monitoring techniques of induction motors. *IEEE transactions on energy conversion*, 20(1):106–114, 2005.

[5] Frédéric Perisse, Piotr Werynski, and Daniel Roger. A new method for ac machine turn insulation diagnostic based on high frequency resonances. *IEEE Transactions on Dielectrics and Electrical Insulation*, 14(5):1308–1315, 2007.

[6] Salem Mgammal Al-Ameri, Ahmed Allawy Alawady, Mohd Fairouz Mohd Yousof, Muhammad Saufi Kamarudin, Ali Ahmed Salem, Ahmed Abu-Siada, and Mohamed I Mosaad. Application of frequency response analysis method to detect short-circuit faults in three-phase induction motors. *Applied Sciences*, 12(4):2046, 2022.

[7] Salem Mgammal Al-Ameri, Ahmed Allawy Alawady, Zulkurnain Abdul-Malek, Zulkarnain Ahmad Noorden, Mohd Fairouz Mohd Yousof, Ali Ahmed Salem, Mohamed Ibrahim Mosaad, and Ahmed Abu-Siada. Frequency response analysis: An enabling technology to detect internal faults within critical electric assets. *Applied Sciences*, 12(18):9201, 2022.

[8] Sandra Plötz, Lukas Ranzinger, and Stephanie Uhrig. Frequency response analysis on rotating machines–model parameterization for different machine types and performance classes. In *2024 International Conference on Diagnostics in Electrical Engineering (Diagnostika)*, pages 01–06. IEEE, 2024.

[9] FR Blánquez, Carlos A Platero, E Rebollo, and F Blánquez. Evaluation of the applicability of fra for inter-turn fault detection in stator windings. In *2013 9th IEEE International Symposium on Diagnostics for Electric Machines, Power Electronics and Drives (SDEMPED)*, pages 177–182. IEEE, 2013.

[10] Salem Mgammal Al-Ameri, Zulkurnain Abdul-Malek, Ali Ahmed Salem, Zulkarnain Ahmad Noorden, Ahmed Allawy Alawady, Mohd Fairouz Mohd Yousof, Mohamed Ibrahim Mosaad, Ahmed Abu-Siada, and Hammam Abdurabu Thabit. Frequency response analysis for three-phase star and delta induction motors: Pattern recognition and fault analysis using statistical indicators. *Machines*, 11(1):106, 2023.

Appendix E

Plagiarism Check Report

Manju Koirala

Thesis Report plag.pdf

Tribhuvan University

Document Details

Submission ID
trn:oid:::3117:451371460

Submission Date
Apr 22, 2025, 12:57 PM GMT+5:45

Download Date
Apr 22, 2025, 1:00 PM GMT+5:45

File Name
Thesis Report plag.pdf

File Size
3.4 MB

46 Pages

10,060 Words

55,684 Characters

5% Overall Similarity

The combined total of all matches, including overlapping sources, for each database.

Match Groups

57 Not Cited or Quoted 5%
Matches with neither in-text citation nor quotation marks

2 Missing Quotations 0%
Matches that are still very similar to source material

0 Missing Citation 0%
Matches that have quotation marks, but no in-text citation

0 Cited and Quoted 0%
Matches with in-text citation present, but no quotation marks

Top Sources

1% Internet sources
5% Publications
0% Submitted works (Student Papers)

Integrity Flags

1 Integrity Flag for Review

Hidden Text
23 suspect characters on 1 page
Text is altered to blend into the white background of the document.

Our system's algorithms look deeply at a document for any inconsistencies that would set it apart from a normal submission. If we notice something strange, we flag it for you to review.

A Flag is not necessarily an indicator of a problem. However, we'd recommend you focus your attention there for further review.

Match Groups

- **57** Not Cited or Quoted 5%
  Matches with neither in-text citation nor quotation marks
- **2** Missing Quotations 0%
  Matches that are still very similar to source material
- **0** Missing Citation 0%
  Matches that have quotation marks, but no in-text citation
- **0** Cited and Quoted 0%
  Matches with in-text citation present, but no quotation marks

Top Sources

1% Internet sources
5% Publications
0% Submitted works (Student Papers)

Top Sources

The sources with the highest number of matches within the submission. Overlapping sources will not be displayed.

1	Publication	Mohammad Sedigh Toulabi, Liwei Wang, Levi Bieber, Shaahin Filizadeh, Juri Jatsk...	<1%
2	Publication	Lukas Ranzinger, Stephanie Uhrig, Stefan Tenbohlen. "Analysis and Modeling the ...	<1%
3	Publication	F. R. Blanquez, Carlos. A. Platero, E. Rebollo, F. Blanquez. "Evaluation of the applic...	<1%
4	Publication	Salem Mgammal Al-Ameri, Ahmed Allawy Alawady, Mohd Fairouz Mohd Yousof, ...	<1%
5	Publication	Muthiah Geethanjali, Hemavathi Ramadoss. "chapter 1 Fault Diagnosis of Inducti...	<1%
6	Internet	umpir.ump.edu.my	<1%
7	Publication	Anik Kumar Samanta, Arunava Naha, Devasish Basu, Aurobinda Routray, Alok Ka...	<1%
8	Publication	M'hamed Drif, Antonio J. Marques Cardoso. "Stator Fault Diagnostics in Squirrel C...	<1%
9	Publication	Trevor Linsley. "Advanced Electrical Installation Work", Routledge, 2019	<1%
10	Publication	Xiao, Yi Qing. "Advanced Macromodeling in the Loewner Framework", McGill Univ...	<1%

11 Internet
ece.au.dk <1%

12 Internet
knowledgecommons.lakeheadu.ca <1%

13 Publication
Mirafzal, Behrooz. "Incipient fault diagnosis in squirrel-cage induction motors", P... <1%

14 Internet
across.fer.hr <1%

15 Publication
Frederic Perisse. "<![CDATA[A New Method for AC Machine Turn Insulation Diagn... <1%

16 Publication
Geoff Klempner, Isidor Kerszenbaum. "Handbook of Large Turbo-Generator Oper... <1%

17 Publication
Das, Santanu, P. Purkait, and S. Chakravorti. "Characterization of short circuit fau... <1%

18 Publication
Zhenyu Zhao, Fei Fan, Wensong Wang, Yong Liu, Kye Yak See. "Detection of Stator... <1%

19 Internet
pumpsinbangalore.blogspot.com <1%

20 Internet
9pdf.net <1%

21 Publication
Lecture Notes in Electrical Engineering, 2015. <1%

22 Publication
Secue, J.R.. "Sweep frequency response analysis (SFRA) for the assessment of win... <1%

23 Publication
Nyanteh, Yaw D., Sanjeev K. Srivastava, Chris S. Edrington, and David A. Cartes. "A... <1%

24 Publication
Fu-yu Lin. "Virtual Impedance Analyzer Design and Implementation", Second Inte... <1%

25 Publication

M. Turzyński. "Induction machine behavioral modeling for prediction of EMI prop... <1%

26 Publication

M.A. Awadallah, M.M. Morcos. "Application of AI tools in fault diagnosis of electri... <1%

27 Publication

D.A. Bradley. "Power Electronics", CRC Press, 2017 <1%

28 Publication

Ian Culbert, John Letal. "Signature analysis for on-line motor diagnostics", 2015 6... <1%

29 Publication

Isidor Kerszenbaum, Geoff Klempner. "Handbook of Large Turbo-Generator Oper... <1%

30 Publication

S.H. Chetwani, M.K. Shah, M. Ramamoorty. "Online condition monitoring of induc... <1%

31 Publication

Li Sheng, Chunyu Li, Ming Gao, Xiaopeng Xi, Donghua Zhou. "A review of SCADA-b... <1%

32 Internet

napier-repository.worktribe.com <1%